

---

NORTH ATLANTIC TREATY  
ORGANISATION



AC/323(SCI-228)TP/446

RESEARCH AND TECHNOLOGY  
ORGANISATION



www.rto.nato.int

---

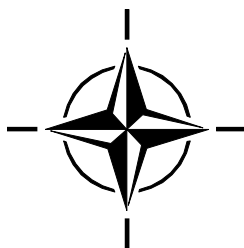
**RTO AGARDograph 160**  
**Flight Test Instrumentation Series – Volume 22**

**SCI-228**

# **Application of Fiber Optic Instrumentation**

(Validation des systèmes d'instrumentation  
à fibres optiques)

This AGARDograph has been sponsored by SCI-228,  
the Flight Test Technology Task Group of the Systems  
Concepts and Integration Panel (SCI) of RTO.



Published July 2012





**RTO AGARDograph 160**  
**Flight Test Instrumentation Series – Volume 22**

**SCI-228**

# **Application of Fiber Optic Instrumentation**

(Validation des systèmes d'instrumentation  
à fibres optiques)

This AGARDograph has been sponsored by SCI-228,  
the Flight Test Technology Task Group of the Systems  
Concepts and Integration Panel (SCI) of RTO.

Authored by

Dr. W. Lance Richards, Ph. D.

Mr. Allen R. Parker, Jr.

Dr. William L. Ko, Ph. D.

Mr. Anthony Piazza

Dr. Patrick Chan, Ph. D.

---

# The Research and Technology Organisation (RTO) of NATO

RTO is the single focus in NATO for Defence Research and Technology activities. Its mission is to conduct and promote co-operative research and information exchange. The objective is to support the development and effective use of national defence research and technology and to meet the military needs of the Alliance, to maintain a technological lead, and to provide advice to NATO and national decision makers. The RTO performs its mission with the support of an extensive network of national experts. It also ensures effective co-ordination with other NATO bodies involved in R&T activities.

RTO reports both to the Military Committee of NATO and to the Conference of National Armament Directors. It comprises a Research and Technology Board (RTB) as the highest level of national representation and the Research and Technology Agency (RTA), a dedicated staff with its headquarters in Neuilly, near Paris, France. In order to facilitate contacts with the military users and other NATO activities, a small part of the RTA staff is located in NATO Headquarters in Brussels. The Brussels staff also co-ordinates RTO's co-operation with nations in Middle and Eastern Europe, to which RTO attaches particular importance especially as working together in the field of research is one of the more promising areas of co-operation.

The total spectrum of R&T activities is covered by the following 7 bodies:

- AVT Applied Vehicle Technology Panel
- HFM Human Factors and Medicine Panel
- IST Information Systems Technology Panel
- NMSG NATO Modelling and Simulation Group
- SAS System Analysis and Studies Panel
- SCI Systems Concepts and Integration Panel
- SET Sensors and Electronics Technology Panel

These bodies are made up of national representatives as well as generally recognised 'world class' scientists. They also provide a communication link to military users and other NATO bodies. RTO's scientific and technological work is carried out by Technical Teams, created for specific activities and with a specific duration. Such Technical Teams can organise workshops, symposia, field trials, lecture series and training courses. An important function of these Technical Teams is to ensure the continuity of the expert networks.

RTO builds upon earlier co-operation in defence research and technology as set-up under the Advisory Group for Aerospace Research and Development (AGARD) and the Defence Research Group (DRG). AGARD and the DRG share common roots in that they were both established at the initiative of Dr Theodore von Kármán, a leading aerospace scientist, who early on recognised the importance of scientific support for the Allied Armed Forces. RTO is capitalising on these common roots in order to provide the Alliance and the NATO nations with a strong scientific and technological basis that will guarantee a solid base for the future.

The content of this publication has been reproduced directly from material supplied by RTO or the authors.

Published July 2012

Copyright © RTO/NATO 2012  
All Rights Reserved

ISBN 978-92-837-0164-4

Single copies of this publication or of a part of it may be made for individual use only. The approval of the RTA Information Management Systems Branch is required for more than one copy to be made or an extract included in another publication. Requests to do so should be sent to the address on the back cover.

---

## AGARDograph Series 160 and 300

Soon after its founding in 1952, the Advisory Group for Aerospace Research and Development (AGARD) recognized the need for a comprehensive publication on Flight Test Techniques and the associated instrumentation. Under the direction of the Flight Test Panel (later the Flight Vehicle Integration Panel, or FVP) a Flight Test Manual was published in the years 1954 to 1956. This original manual was prepared as four volumes: 1. Performance, 2. Stability and Control, 3. Instrumentation Catalog, and 4. Instrumentation Systems.

As a result of the advances in the field of flight test instrumentation, the Flight Test Instrumentation Group was formed in 1968 to update Volumes 3 and 4 of the Flight Test Manual by publication of the Flight Test Instrumentation Series, AGARDograph 160. In its published volumes AGARDograph 160 has covered recent developments in flight test instrumentation.

In 1978, it was decided that further specialist monographs should be published covering aspects of Volumes 1 and 2 of the original Flight Test Manual, including the flight testing of aircraft systems. In March 1981, the Flight Test Techniques Group (FTTG) was established to carry out this task and to continue the task of producing volumes in the Flight Test Instrumentation Series. The monographs of this new series (with the exception of AG237 which was separately numbered) are being published as individually numbered volumes in AGARDograph 300. In 1993, the Flight Test Techniques Group was transformed into the Flight Test Editorial Committee (FTEC), thereby better reflecting its actual status within AGARD. Fortunately, the work on volumes could continue without being affected by this change.

An Annex at the end of each volume in both the AGARDograph 160 and AGARDograph 300 series lists the volumes that have been published in the Flight Test Instrumentation Series (AG 160) and the Flight Test Techniques Series (AG 300) plus the volumes that were in preparation at that time. Annex B of this paper reproduces current such listings.

---

# Application of Fiber Optic Instrumentation

(RTO AG-160 Vol. 22 / SCI-228)

## Executive Summary

This AGARDograph presents an introduction to fiber optic systems and is intended to provide a basic understanding of the utilization of these systems for aircraft instrumentation. It documents the current state of the art and provides references for users of this technology to track the rapid advances expected in fiber optic technology in the coming years.

Revolutionary advances in fiber optic technology, as applied to flight-test instrumentation, have been achieved over the last decade and are expected to continue at a rapid pace for the foreseeable future. There has been significant maturation in both the manufacturing of fibers and the miniaturization of hardware, which has enabled movement of this technology from controlled laboratory environments to realistic aircraft operations. The ability to closely space sensors on the fibers has improved by orders of magnitude and the capability for continuous sensors is rapidly becoming feasible. Fiber optic systems will revolutionize flight-test instrumentation for all of the NATO members, potentially eliminating strain gages and their associated wiring while collecting more accurate and densely spaced measurements at a significantly reduced system weight. Fiber optic instrumentation provides the ability to capture system-wide stress, strain, and temperature measurements far beyond classic aircraft flight-test instrumentation applications. The technology also enables the determination of many other derived engineering parameters such as structural shape, and applied loads; information that has not been available before with conventional aircraft sensors systems.

This AGARDograph documents the current state of the art for this technology and provides references for users to track the rapid advances expected in fiber optics in the coming years. One application for this technology could be to a wide range of NATO aircraft systems in order to establish a comprehensive set of data for aging aircraft. Other future applications could entail embedding fiber optic systems in composite structures as they are manufactured, allowing extremely light-weight flexible structures to be actively controlled, giving enhanced capability to air, surface, and ground-based NATO systems.

# Validation des systèmes d'instrumentation à fibres optiques

(RTO AG-160 Vol. 22 / SCI-228)

## Synthèse

Cette AGARDograph présente une introduction aux systèmes à fibres optiques et a pour objet d'expliquer l'utilisation de ces systèmes dans l'instrumentation embarquée. Elle expose l'état actuel de la technique et fournit un cadre de référence pour que les utilisateurs de cette technologie puissent suivre les progrès rapides qui sont attendus dans le domaine des fibres optiques au cours des années à venir.

Durant les dix dernières années, des progrès révolutionnaires ont été accomplis par la technologie des fibres optiques appliquée à l'instrumentation des essais en vol, et ces avancées devraient se poursuivre à un rythme rapide dans un avenir prévisible. Le degré de maturité des procédés de fabrication de fibres et de miniaturisation du matériel a progressé, permettant ainsi à cette technologie de passer du stade des conditions contrôlées en laboratoire au stade des conditions d'opérations aériennes réalistes. La densité d'intégration de capteurs dans les fibres a été accrue de plusieurs ordres de grandeur et les progrès réalisés en termes de faisabilité de capteurs continus sont rapides. Les systèmes à fibres optiques vont révolutionner l'instrumentation des essais en vol dans l'ensemble des pays membres de l'OTAN, entraînant la disparition progressive des jauges extensométriques et des câblages qu'elles nécessitent, tout en autorisant des mesures plus précises à haute densité d'intégration et pour un poids bien moindre. Les instruments à fibres optiques offrent des capacités de mesure de contrainte, d'allongement et de température à l'échelon d'un système bien supérieures aux possibilités des instruments embarqués classiques d'essais en vol. Grâce à cette technologie, il est en outre possible de calculer une multitude d'autres paramètres techniques dérivés, tels que la forme de structures et les charges appliquées, informations qu'il n'était jusqu'à présent pas possible de recueillir avec les systèmes de capteurs embarqués classiques.

Cette AGARDograph expose l'état actuel de la technique et fournit un cadre de référence pour que les utilisateurs de cette technologie puissent suivre les progrès rapides qui sont attendus dans le domaine des fibres optiques au cours des années à venir. Cette technologie pourrait, notamment, être appliquée à un large éventail de systèmes d'aéronefs de l'OTAN dans le but de constituer un ensemble détaillé de données pour des aéronefs vieillissants. D'autres applications futures pourraient consister à intégrer des systèmes à fibres optiques dans des structures composites en cours de fabrication, autorisant ainsi le contrôle actif de structures flexibles ultra légères et améliorant les capacités des systèmes OTAN aériens, de surface et terrestres.

---

## Acknowledgements

The authors gratefully acknowledge the support provided by our many colleagues at NASA Dryden Flight Research Center and across the agency who have provided seemingly endless opportunities to validate fiber optic sensing technology on a wide variety of aerospace vehicles and large-scale test articles. We are greatly indebted to the highly-qualified technical staff in the Flight Loads Laboratory at NASA Dryden for their expertise in conducting the large-scale structural test operations. These tests were essential to validate many of the new theories and measurement approaches documented in this report. We are especially grateful for the encouragement, strong support and technical leadership provided by our senior management for allowing us the opportunity to help mature this technology for NASA applications. Special thanks go to Mr. Patrick Stoliker for the many years of technical guidance he provided as Director for Research, as well as his unflinching support as Deputy Center Director to publish the technical results in this report.



# Table of Contents

	<b>Page</b>
<b>AGARDograph Series 160 and 300</b>	<b>iii</b>
<b>Executive Summary</b>	<b>iv</b>
<b>Synthèse</b>	<b>v</b>
<b>Acknowledgements</b>	<b>vi</b>
<b>List of Figures/Tables</b>	<b>ix</b>
<b>List of Acronyms and Symbols</b>	<b>xi</b>
<b>Preface</b>	<b>xiii</b>
<b>Chapter 1 – Introduction</b>	<b>1-1</b>
<b>Chapter 2 – Background</b>	<b>2-1</b>
2.1 Merits of Fiber Optic Sensors	2-1
2.1.1 Weight	2-1
2.1.2 Multiplexing	2-2
2.1.3 Embedment	2-3
2.1.4 Safety	2-4
2.2 FBG Theory	2-4
2.3 Optical Frequency Domain Reflectometry	2-6
<b>Chapter 3 – System Development</b>	<b>3-1</b>
3.1 Ground-Based Interrogation Systems	3-1
3.2 Flight-Based Interrogation Systems	3-1
<b>Chapter 4 – Sensor Characterization and Attachment</b>	<b>4-1</b>
4.1 FBG Transverse Sensitivity	4-1
4.2 FBG Temperature Sensitivity	4-1
4.3 Advanced Surface-Mounted Installation Methods	4-3
4.4 Advanced Embedded Installation Methods	4-4
<b>Chapter 5 – On-Board Structural Transfer Functions</b>	<b>5-1</b>
5.1 Wing Shape	5-1
5.1.1 NASA Dryden Real-Time Data-Driven Displacement Methods	5-1
5.1.1.1 Theory	5-2
5.1.1.2 Formulation	5-2

---

5.1.1.3	Implementation	5-3
5.1.2	NASA LaRC/Dryden Displacement Theory	5-3
5.2	Structural Properties and External Loads	5-5
5.3	Fatigue Life	5-6
<b>Chapter 6 – Recent Examples of Large Scale FOSS Testing</b>		<b>6-1</b>
6.1	NESC – Composite Crew Module Structural Testing	6-1
6.2	Ikhana	6-2
6.2.1	Sensor Attachment	6-3
6.2.2	Ground Testing	6-4
6.3	Global Observer	6-5
6.3.1	Flight Testing	6-5
6.3.2	Wing-Load Testing	6-6
<b>Chapter 7 – The Future of FOSS and FBG-OFDR Technologies</b>		<b>7-1</b>
7.1	The FOSS Vision Vehicle	7-1
7.2	Design and Development	7-2
7.3	Fabrication and Sensor Installation	7-3
7.4	Ground Testing	7-3
7.5	Flight Operations	7-4
7.5.1	Nominal Flight	7-4
7.5.2	Off-Nominal Flight	7-5
7.6	End of Life Decision Making	7-5
<b>Chapter 8 – Conclusions</b>		<b>8-1</b>
<b>Chapter 9 – References</b>		<b>9-1</b>
<b>Annex A – AGARD and RTO Flight Test Instrumentation and Flight Test Techniques Series</b>		<b>A-1</b>
1.	Volumes in the AGARD and RTO Flight Test Instrumentation Series, AGARDograph 160	A-1
2.	Volumes in the AGARD and RTO Flight Test Techniques Series	A-3

## List of Figures/Tables

<b>Figure</b>		<b>Page</b>
Figure 2-1	Comparison of Typical Installations of Strain Gages, and a Fiber Optic Sensor	2-2
Figure 2-2	Comparison of Typical High Temperature Installations of a Strain Gage, and a Fiber Optic Sensor	2-2
Figure 2-3	Instrumentation Comparison Between Strain Gage and Fiber Optic Sensor Technology	2-3
Figure 2-4	FBG Sensors Embedded in Composite Structures	2-4
Figure 2-5	Reflected and Transmitted Light Through a Bragg Grating	2-5
Figure 2-6	Schematics of a Typical OFDR System	2-6
Figure 2-7	Fiber with Multiple Bragg Gratings	2-6
Figure 2-8	Fiber Optical Network with Reference Arm	2-7
Figure 2-9	Fourier Transform from Wavelength to Spatial Domain to Discern Between Gratings	2-7
Figure 2-10	Window Function and Inverse Fourier Transform from Spatial to Wavelength Domain	2-8
Figure 3-1	Ground-Based 4-Fiber Interrogation System	3-1
Figure 3-2	Flight 4-Fiber Interrogation System and Predator B Aircraft	3-2
Figure 3-3	Environmental Qualification Requirements and System Design for the Ikhana Flight System	3-3
Figure 4-1	Typical Installation for Measuring Strain and Temperature	4-2
Figure 4-2	Installation of FBG Fiber on Wing Upper Surface of Dryden's Predator-B UAV	4-3
Figure 4-3	Typical Collocated Cross-Section with Conventionally Bonded FBG, Conventional Foil Strain Gage, and FBG Incorporated into the SMART Layer	4-4
Figure 5-1	Helios UAV (AeroVironment Inc.)	5-2
Figure 5-2	Tapered Wing Box Instrumented with Two-Line Strain-Sensing System	5-3
Figure 5-3	Three-Core Fiber and Three Single-Mode Fibers Arranged 120° Apart	5-4
Figure 5-4	Finite-Element Model	5-6
Figure 5-5	Analytically Determined Loads	5-6
Figure 5-6	Typical Crack Growth Curve for B-52 Pylon Front Hook	5-7
Figure 6-1	Ground-Based Four-Fiber Interrogation System and NESC CCM Testing	6-1
Figure 6-2	Sample Real-Time Measurement Data of the Fiber Sensor versus Simulation Result of the Left-Side Window of the CCM During Maximum Internal Pressure Load	6-2
Figure 6-3	Ikhana UAV Vehicle with Sensors Installed; in Flight Prior to Experiment	6-3
Figure 6-4	FBG Sensor Layout	6-3
Figure 6-5	Ikhana Ground Testing	6-4
Figure 6-6	Ikhana Flight-Test Data	6-5
Figure 6-7	Flight Interrogation Unit and the Global Observer UAV	6-6

---

Figure 7-1	Helios UAV at Take-Off and In-Flight Break-Up	7-3
Figure 7-2	Traditional Strain Gage Loads Calibration Testing in NASA Dryden's Flight Loads Lab, and Simplified Tests for Determining Structural Properties of as Built Structures and Real Time in Flight Loads	7-4
Figure 7-3	B52 Aircraft Boneyard, and Video Capture of an In-Flight Structural Failure of a C-130A	7-6

<b>Table</b>		<b>Page</b>
Table 2-1	Strain and Temperature Measurements as Critical Health and Usage Monitoring Parameters	2-1

## List of Acronyms and Symbols

A/D	Analog to Digital
ATR	Air Transport Rack
$c$	half depth of uniform beam (distance from neutral surface to bottom or top surface), in.
CCM	Composite Crew Module
cPCI	compact Peripheral Component Interconnect
COPV	Composite Over-wrapped Pressure Vessel
COTS	Commercial-Off-The-Shelf
CPU	Central Processing Unit
DUT	Device Under Test
$E$	Young modulus, lb/in <sup>2</sup>
EFPI	Extrinsic Fabry Perôt Interferometer
EMI	Electromagnetic Interference
EMP	Electromagnetic Pulse
FBG	Fiber Bragg Grating
FEA	Finite Element Analysis
FLL	Flight Loads Laboratory
FOSS	Fiber Optic Smart Structure
$I$	moment of inertia, in <sup>4</sup>
$I_R$	reflected intensity of light
$k$	wave number
$L$	optical path length difference
$n_0$	core index of refraction
$n$	effective index of refraction
NASA	National Aeronautics and Space Administration
NESC	NASA Engineering Safety Center
O/E	Optical to Electrical
OFDR	Optical Frequency Domain Reflectometry
$p_e$	strain-optic coefficient
$P$	applied load, lb
$R$	spectrum of $i^{th}$ grating
$S$	Section modulus, I/c, in <sup>3</sup>
$T$	Temperature, °F
UAV	Uninhabited Aerial Vehicle

---

$\alpha$	coefficient of thermal expansion
$\alpha_n$	thermal optic coefficient
$\alpha_{sub}$	thermal optic coefficient substrate
$\alpha_A$	coefficient of thermal expansion of fiber
$\varepsilon$	strain, $\mu\text{in/in}$
$\varepsilon_{app}$	apparent strain, $\mu\text{in/in}$
$\varepsilon_{ind}$	indicated strain, $\mu\text{in/in}$
$\varepsilon_{true}$	true strain, $\mu\text{in/in}$
$\delta$	multidimensional differential operator
$\Delta$	one dimensional change in scalar value
$\Delta l$	distance between two adjacent strain-sensing stations, in
$\lambda$	light wavelength, nm
$\lambda_B$	Bragg reflected wavelength, nm
$\Lambda$	periodity of grating planes
$\xi$	temperature coefficient of resistivity

## Preface

Dr. W. Lance Richards has a Ph.D. in mechanical engineering from the University of Wales, Swansea, UK. He has 30 years experience with NASA conducting research, development, and implementation of advanced sensors and instrumentation, with specific application to aerospace vehicle technology. He has authored more than 75 reports and is a co-recipient of U.S. patents for developing highly accurate and efficient data-driven methods for real-time, on-board determination of structural shape and externally-applied loads for aerospace vehicles.

Allen R. Parker Jr. received a Master of Engineering degree in the area of microelectronics from Texas A&M University. Mr. Parker is currently working as a researcher at NASA's Dryden Flight Research Center focusing in the area of advanced sensor development with major emphasis on using fiber Bragg gratings to measure various physical parameters. He has played a major part in the development of algorithms and systems, which has made possible the practical application of this "game changing" sensing technology. With this technology, Mr. Parker continues to support projects inside as well as outside NASA, covering industries from medical to aerospace to space.

Dr. William L. Ko has a Ph.D. degree in aeronautics from California Institute of Technology. He formulated the internationally recognized Blatz-Ko Constitutive Law for hyperelastic materials. He also formulated aging theories for flight structure service life predictions. Lately, he developed displacement theories for converting surface strains into out-of-plane deflection for deformed shape predictions of aerospace structures.

Anthony Piazza has over 25 years experience in the field of structural instrumentation and test; specializing in strain measurements using both electrical and optical based sensors/systems. He also possesses unique proficiency in the development, attachment, evaluation, and characterization of extreme sensors applicable to hot-structures testing and hostile environments.

Dr. Patrick Hon Man Chan has a Ph.D. in Interdisciplinary Material Science and Engineering from University of California, Irvine. He is a fiber optics researcher at NASA Dryden, working to mature various aspects of current fiber optics sensing system technology for wide-spread deployment. Dr. Chan has published numerous journal papers related to fiber technology, and is currently working on all-fiber laser source as well as conducting research on shape-sensing fiber technology.





## Chapter 1 – INTRODUCTION

A new technology has emerged in recent years that has the potential to dramatically improve the design and efficient operation of aerospace vehicles throughout their entire life cycle, from initial design to final retirement. This new technology, often referred in the literature as Fiber Optic “Smart” or “Sensory” Structures (FOSS), began in the early 1980s with breakthroughs in the miniaturization of sensors and actuators, along with advances made in the field of composite materials. The FOSS concept, as originally envisaged, involved the distribution of advanced sensor networks, such as fiber optic sensors, that could be integrated within, and adhered to the surface of load-bearing composite structures. The vision was that these sensors could be distributed in vast networks analogous to the nervous system in the human body. Information from these sensory networks could be fed-back to on-board or central processing computers, serving as the brain, which in turn could provide instructive information to pilots, maintenance crews, or other key decision makers responsible for ensuring vehicle performance over the vehicle’s life cycle. Stresses, structural instabilities, temperature distributions, and a plethora of other engineering measurands could be monitored in real time with a single fiber optic based instrumentation system. Such a system could offer an unparalleled amount of valid engineering data indicating the structure and sub-system health with almost no weight penalty.

While an increasing number of FOSS technologies are emerging from the research laboratory, many technological barriers still exist that impede its acceptance by the aerospace community. This acceptance is especially challenging because of strict vehicle performance requirements, coupled with highly aggressive project schedules that compete against the implementation of what is viewed by many as “high risk” technologies. Much of that risk comes from a lack of understanding of the accuracy and performance of embedded sensors in large-scale FOSS components. This area must be addressed and the integration risk reduced by thoroughly validating the new technology using universally accepted industrial standards. A greater emphasis on large-scale sensor validation is required before FOSS components can gain full acceptance by the mainstream engineering community and placed into service.

While some of the barriers toward FOSS application are technical, many of these barriers are cultural. As with any new technology, the fear of change from what works, no matter how antiquated, to what could be involves a cultural paradigm shift from conventional thinking. Without these cultural changes, realizing the benefits of FOSS technologies could have the real consequence of limiting the efficiency and performance of future aircraft vehicle designs. Or far worse, a failure to embrace the advantages of new promising technologies, such as FOSS could impair competitiveness in combat or impact economic competitiveness in the global marketplace.

To address these barriers, this paper first presents work that has been conducted at the National Aeronautics and Space Administration (NASA) Dryden Flight Research Center (Edwards, California) to clear some of the FOSS technical barriers to large-scale application. After a brief overview of conventional and fiber optic sensor technology, an overview of the research and development that has been conducted using fiber optic sensors at all vehicle phases will be discussed. Lastly, to help overcome the cultural resistance, the FOSS vision is presented and its potential benefits in aerospace vehicle design throughout the life cycle are presented.



## Chapter 2 – BACKGROUND

Strain gage measurements are the industry standard for determining the state-of-stress of a structure, quantifying airframe loads to evaluate if airframe load limits have been exceeded, or for calculating the remaining available airframe fatigue life. The foil strain gage is extremely accurate, reliable, economical, easy to use, exceptionally linear, highly repeatable, and possesses a very strong signal-to-noise ratio. As shown in Table 2-1, strain and temperature measurements are the most basic of all structural parameters and can be used to quantify many types of airframe failures (W. Sheppard, “SHM Flight Test Panels, Sensor Integration, Rev 3”, project files, 2002).

**Table 2-1: Strain and Temperature Measurements as Critical Health and Usage Monitoring Parameters.**

Failure Mode	Structural Health Monitoring Sensor
Leaks	Gas detection/temperature
Disbond/delaminations	Strain/temp/acousto-ultrasonics/acoustic emission
Thermal protection failure	Strain/temperature
Overloads	Strain
Over pressure	Strain/pressure
Thermal damage	Temperature / strain / gas detection
Dynamic overloads	Acceleration / dynamic strain
Impact damage	Acoustic emission/train
Moisture/corrosion	Humidity sensor

The major drawbacks of conventional strain and temperature sensor technology are with its heavy wire weight, large bundle sizes, and that the technology provides only local measurements in very near proximity to the sensing region. Advanced sensing technology, such as distributed Bragg grating sensors, avoids some of the limitations of conventional measurements by providing enormous numbers of engineering parameters, such as strain, temperature, and structural shape, with a minimal weight penalty that cannot be matched by any other current sensing technology. Fiber optic sensors also have a safety advantage because they are chemically inert and, unlike conventional sensors, are immune to electromagnetic interference and are not susceptible to sparking or Joule heating. Because of their small size, these sensors can also be embedded within composite materials. Additional references to fiber optic sensing, smart structures, and fiber optic structural health monitoring can be found in the literature. [1-5]

### 2.1 MERITS OF FIBER OPTIC SENSORS

#### 2.1.1 Weight

The primary reason for the popularity of fiber optic sensors resides in their weight. They are extremely light and are about the size of a human hair. This is an especially attractive feature for the aerospace community, where weight is crucial to mission and/or commercial success. As an example, Figure 2-1 shows a comparison between a typical strain gage installation and an analogous fiber optic sensor. In this example, the strain gage sensor itself is heavier and for most installations requires three copper lead wires to connect to

## BACKGROUND

the data acquisition system. As will be explained in the next section, hundreds of fiber optic sensors can be located on one optical fiber. Therefore, considerable weight savings can be gained based on the sensor-to-sensor comparison as well as the sensor-to-lead wire efficiency gained by the fiber optic sensor. A typical installation is 0.1 to 1% the weight of conventional gage installations (based on past trade studies).

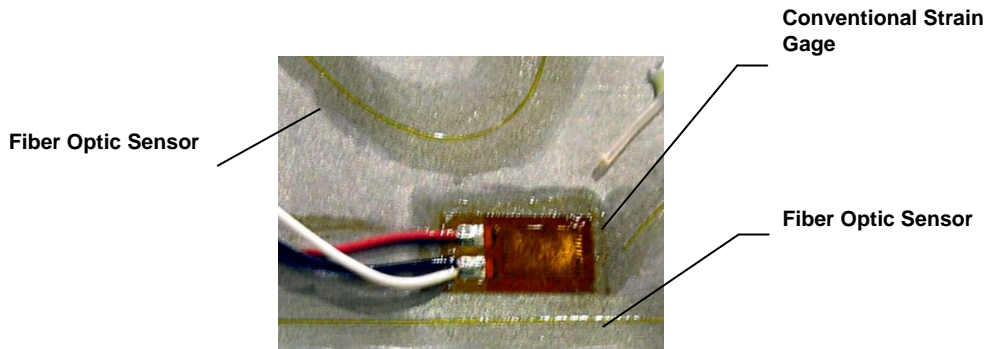


**Figure 2-1: Comparison of Typical Installations of Strain Gages, and a Fiber Optic Sensor.**

This comparison becomes even more dramatic when one compares the state-of-the-art for conventional high temperature metallic strain gages with an equivalent fiber optic sensor (Figure 2-2). For aerospace applications these weight savings have direct correspondence to increases in payloads that vehicles can deliver, and significantly extend the range at which they can travel.

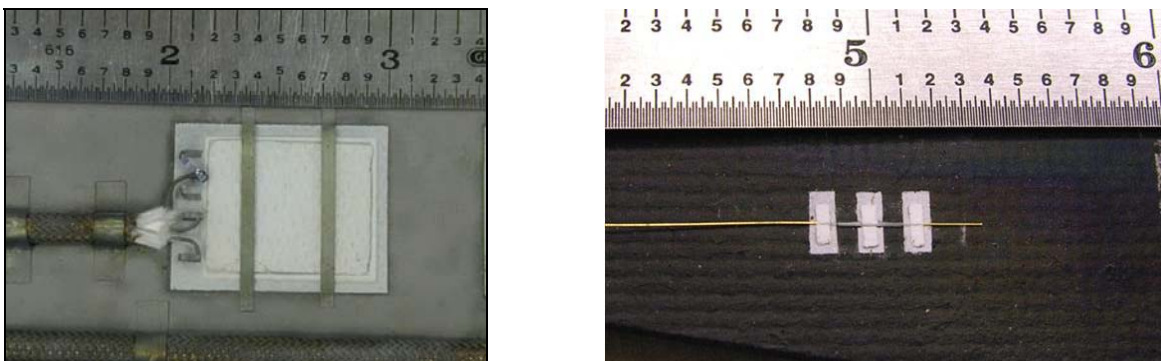


**Figure 2-2: Comparison of Typical High Temperature Installations of a Strain Gage (Left), and a Fiber Optic Sensor (Right).**

### 2.1.2 Multiplexing

In an industry where weight alone can be sufficient justification to incorporate a new technology, weight is only a small part of the Fiber Bragg Gratings (FBG) advantage. The real strength of the FBG resides in its capability to be multiplexed serially. This means that a single optical fiber can contain thousands of discrete FBG sensors along its length using the Optical Frequency Domain Reflectometry (OFDR) multiplexing scheme. For example, a recent flight test program at NASA Dryden conducted on a Predator-B (General Atomics Aeronautical Systems, Incorporated, San Diego, California) successfully flew a FBG system with six optical fibers, each containing approximately 500 fiber optic sensors. [6] Each of these sensors produced a measurement every 0.5 inch that was analogous to the discrete measurement provided by a strain gage at a fraction of the weight.

Multiplexing also provides benefits by dramatically reducing sizes of cable bundles and reducing the complexity of integration and testing of large-scale structural components. Figure 2-3 shows a dramatic comparison between conventional sensors and FBG technology for a ground test article and a flight test fixture. The flight test fixture was instrumented with both conventional and fiber optic sensors and flown at NASA Dryden Flight Research Center. [7] Lead wires from 32 strain gages are shown next to 5 optical fibers containing the same number of fiber optic sensors. (The strain gage instrumentation is shown as white and red jacketed lead wires, and the 5 optical fibers are visible on the left in purple.) This multiplexing advantage saves considerable amounts of time required for pre-flight installation, integration, and identification and trouble-shooting.

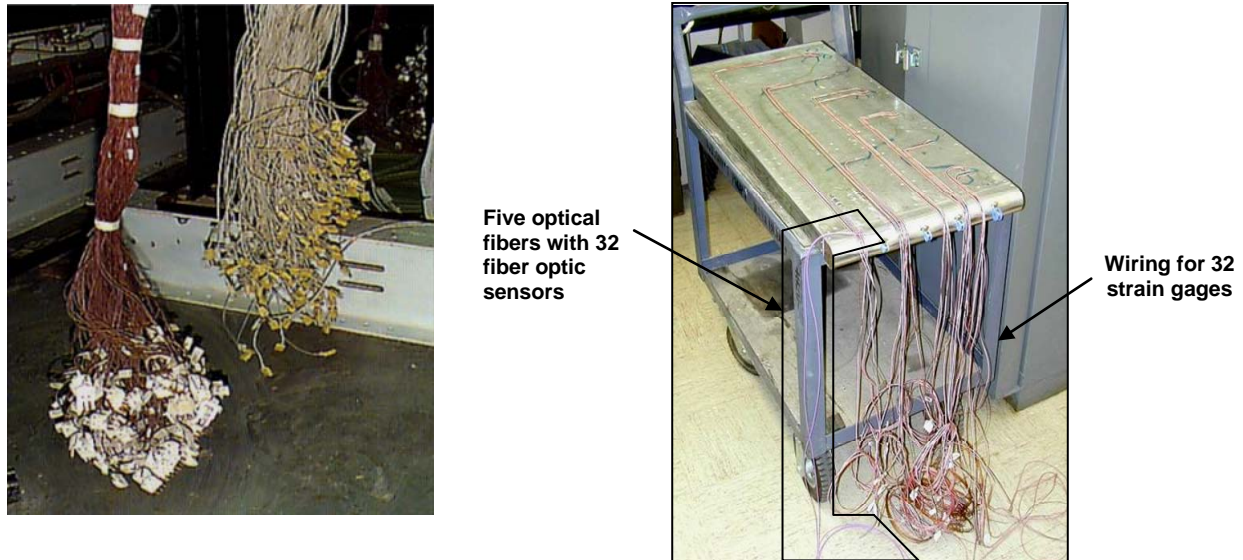


**Figure 2-3: Instrumentation Comparison Between Strain Gage and Fiber Optic Sensor Technology.**

### 2.1.3 Embedment

In addition to what has been mentioned previously about the small size of fiber optic sensors, this advantage means that it is more readily embedded within advanced composite materials. By inspection the cylindrical shape of the fiber sensor is clearly more conducive to embedding with composites because of its smooth non-intrusive geometry. This physical characteristic enables internal strain field measurement of complex material systems during the manufacturing process and testing. Figure 2-4 (left) shows a strain plot of FBG sensors embedded under the load-introduction device on the composite crew model structure called the CM-ALAS. The strain fields measured under the bolted joint were correlated with finite element predictions. Figure 2-4 (right) shows a composite shear panel during testing. This panel had 16 embedded fiber optic sensors that could be correlated with conventional sensors on the front and back of the structure.

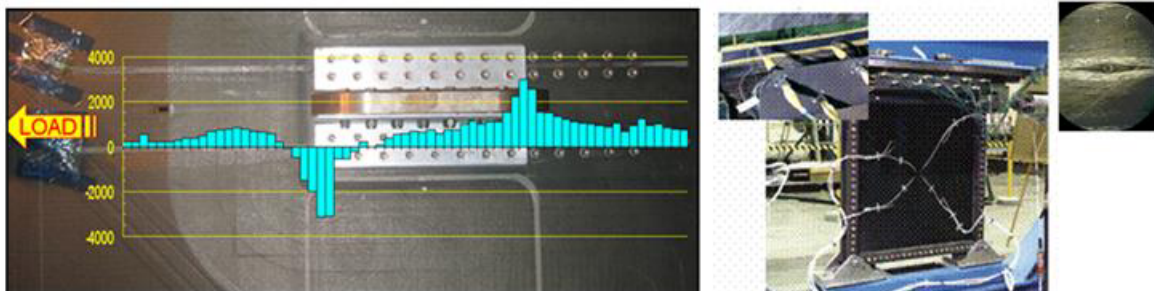


**Figure 2-4: FBG Sensors Embedded in Composite Structures. Strain measurements from FBGs embedded under bolted joint on the composite crew module panel (left), and fiber optic sensors embedded in 2 ft by 2 ft shear panel (right).**

The ability to embed has also led to technical challenges that have limited its application to aerospace structures. The issue of fiber ingress/egress from the composite has created technical challenges, which are the subject of ongoing research and development tasks. The measurement interpretation of embedded FBGs also hampers its acceptance. [8, 9] Interpreting measurements from FBGs embedded in composites is a multi-disciplinary problem. Expertise in sensor and measurement technology, structural mechanics, experimental stress analysis, composite materials, interrogation systems, and optics are all required to adequately understand these measurements while acquired from within complex materials systems.

#### **2.1.4 Safety**

Fiber optic sensors are also inherently safer than conventional sensors. Hermetically coated glass is chemically inert, not susceptible to corrosion, and does not have potential for ground loops, electrical faults, sparking, or Joule heating. These sensors also are not negatively impacted like common aircraft avionics systems with reactions to Electro-Magnetic Interference (EMI) or Electro-Magnetic Pulses (EMP).

### **2.2 FBG THEORY**

Fiber Bragg Gratings (FBG) are produced in optical fibers, which consist of a silica glass cylindrical shaped core, surrounded by a silica cladding of slightly higher index of refraction, and a protective coating. The differences in indices of refraction between the core and the cladding create a waveguide, which as the name implies, serves to efficiently guide light waves down the core of the fiber.

FBGs are created by exposing an optical fiber to an ultraviolet interference pattern, which produces a periodic change in the core index of refraction. [10] These periodic changes cause a reflection when the light in the waveguide is of a particular wavelength while other wavelengths are transmitted in the fiber, as shown in Figure 2-5. The particular reflected wavelength, known as the Bragg wavelength ( $\lambda_B$ ) is dependent upon the FBG's period of core index modulation ( $\Lambda$ ) and the effective core index of refraction ( $n_0$ ).

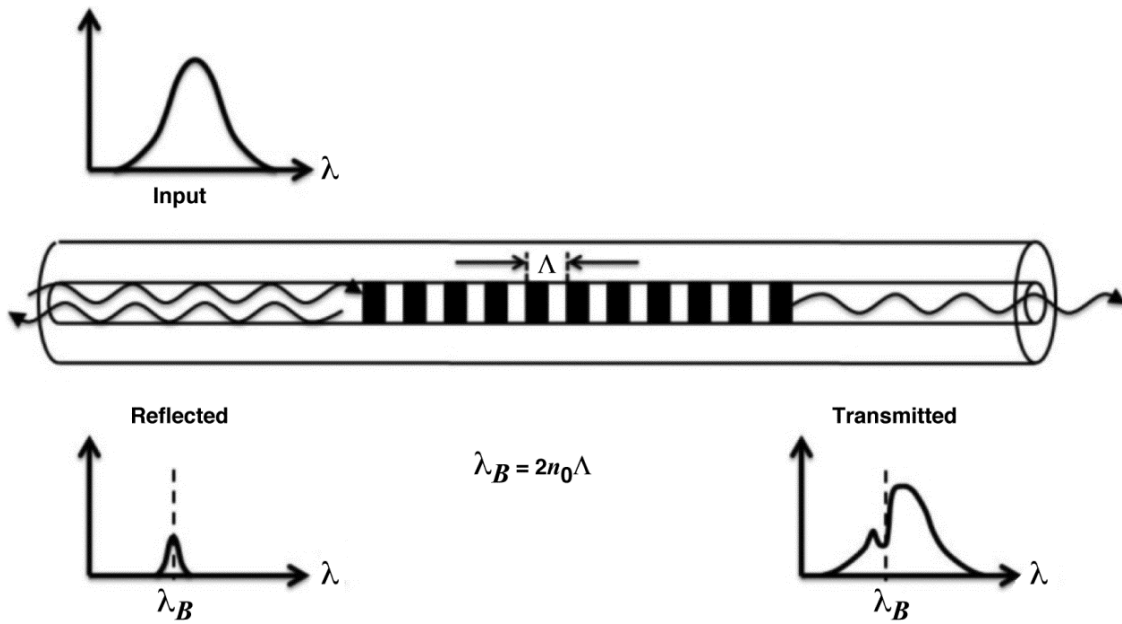


Figure 2-5: Reflected and Transmitted Light Through a Bragg Grating.

When the FBG is strained along the fiber axis, the Bragg grating stretches or contracts, causing  $\Lambda$  and  $n_0$  to increase or decrease. This, in turn, produces an increase or decrease (i.e.  $\delta$ ) in  $\lambda_B$  directly related to  $\Lambda$  and  $n_0$  as represented in equation (1).

$$\delta\lambda_B = \delta(2n_0\Lambda) = 2\Lambda(\delta n_0) + 2n_0(\delta\Lambda) \quad (1)$$

Assuming the strain is constant along the length of the Bragg grating, the change in  $\Lambda$  relates to the kinematic stretch of the fiber and in turn, relates to strain. The relationship between strain and change in index of refraction is determined using a strain-optic tensor comprised of photoelastic coefficients. The number of independent coefficients in the strain-optic tensor is reduced under the assumption that the fiber is optically isotropic, and the set of equations collapses to a single expression shown in equation (2) when the strain field is predominantly uniaxial along the fiber-grating axis.

$$\left[ \frac{\Delta\lambda_B}{\lambda_B} \right] = (1 - p_e)\varepsilon + (\alpha_\Lambda + \alpha_n)\Delta T \quad (2)$$

where  $\Delta\lambda_B$  is the change in Bragg wavelength,  $\lambda_B$  is the unstrained Bragg wavelength,  $p_e$  is a reduced, first order strain-optic coefficient,  $\varepsilon$  is the strain in the fiber direction,  $\alpha_\Lambda$  is the coefficient of thermal expansion of the fiber, and  $\alpha_n$  is the thermal-optic coefficient. Temperature measurements are made with FBGs by decoupling the strain field from the substrate by placing the fiber in a small tube and attaching the tube to the substrate. The tube allows the FBG to freely expand in the tube during loading. In this case, all terms but  $\alpha_n\Delta T$  on the right side of the equation are zero. Pure mechanical strain is determined by bonding the FBG directly to the substrate and employing conventional temperature correction techniques established for strain gages. [11]

A typical optical fiber used in our research is single-mode with a cladding diameter of 127  $\mu\text{m}$  and polyimide coating thickness of 7  $\mu\text{m}$ . Each optical fiber contained multiple FBGs equally spaced with Bragg wavelengths of approximately 1546 nm and strain-optic coefficients,  $p_e$ , of 0.1667.

### 2.3 OPTICAL FREQUENCY DOMAIN REFLECTOMETRY

The system used at NASA Dryden is based on the Langley method using OFDR to interrogate FBG. Typical OFDR systems interpret a beat frequency between a reference arm and the sensing arm where the Device Under Test (DUT) is located; usually the interfering signal is generated through a Michelson interferometer. Figure 2-6 is a schematic of a typical OFDR system in a Michelson interferometer, composed of a wavelength-tunable laser (wavelength-swept laser) at ~1550 nm, a square-law photodiode detector, and two broadband reflective mirrors.

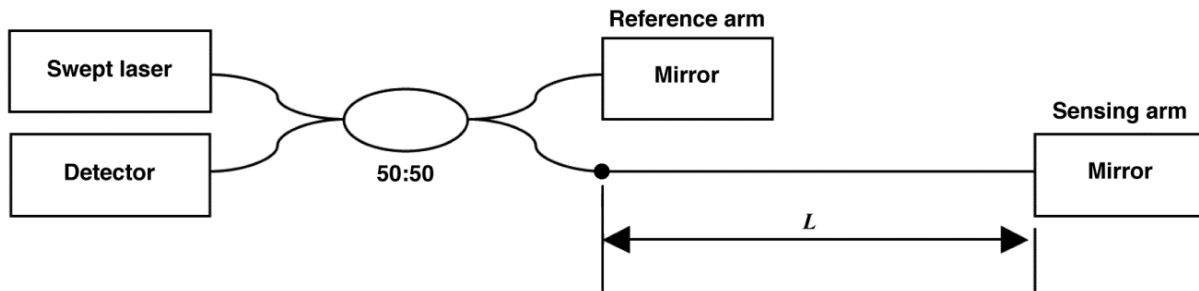


Figure 2-6: Schematics of a Typical OFDR System.

First, a tunable laser acts as a probe signal by continuously sweeping a predetermined frequency range. Light then travels through a 50:50 (2 x 2) fiber coupler, where light of equal intensity will then be reflected from each arm by a broadband reflector (mirror). Signals from both arms will be recombined by the fiber coupler; however, there is a corresponding phase difference (delay) between the reference arm and the sensing arm due to the path length difference L. The combined signal will interfere with one another due to this phase difference, where the intensity of the interfering signal will then be detected by the photodetector.

This same interference effect is applied to Bragg gratings used as strain sensors (Figure 2-7). In OFDR application of these sensors, the distance of each sensor can be individually determined first through sampling of output intensity while sweeping the laser's wavelength at all wavelength ranges. The output intensity/signal is a summation of the complete set of gratings located along the fiber length. Each grating is modulated with its unique frequency, a frequency that is determined by the grating's unique position on the fiber. These sensors are attached to an optical network for inspection.

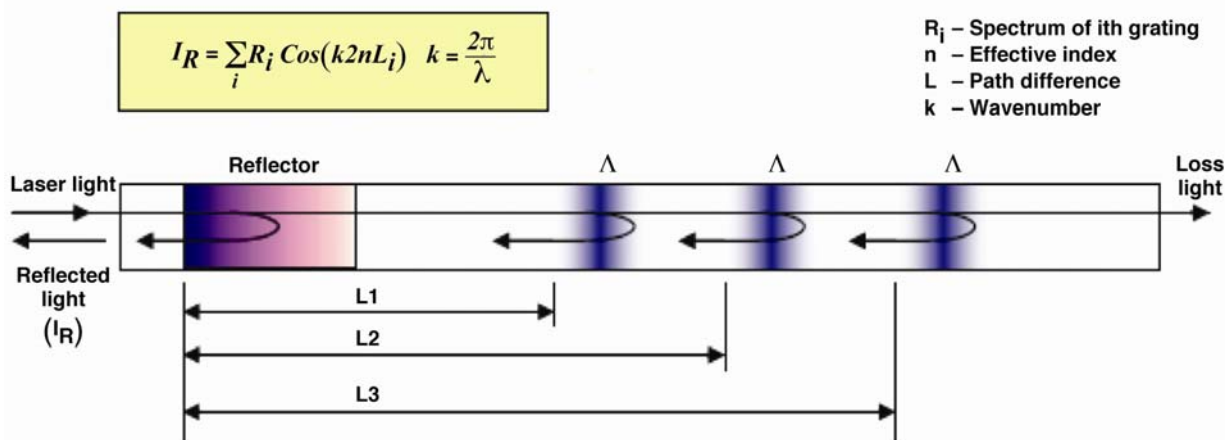


Figure 2-7: Fiber with Multiple Bragg Gratings.



Figure 2-8 illustrates the implementation of an optical network used to interrogate 4 fibers simultaneously. The tunable laser provides excitation for both the sensing and reference part of the network with 95% of its light to be partitioned equally among the four sensing arms. The remaining 5% is sent into a Michelson interferometer to generate a necessary sampling clock by which the four sensor arms are sampled.

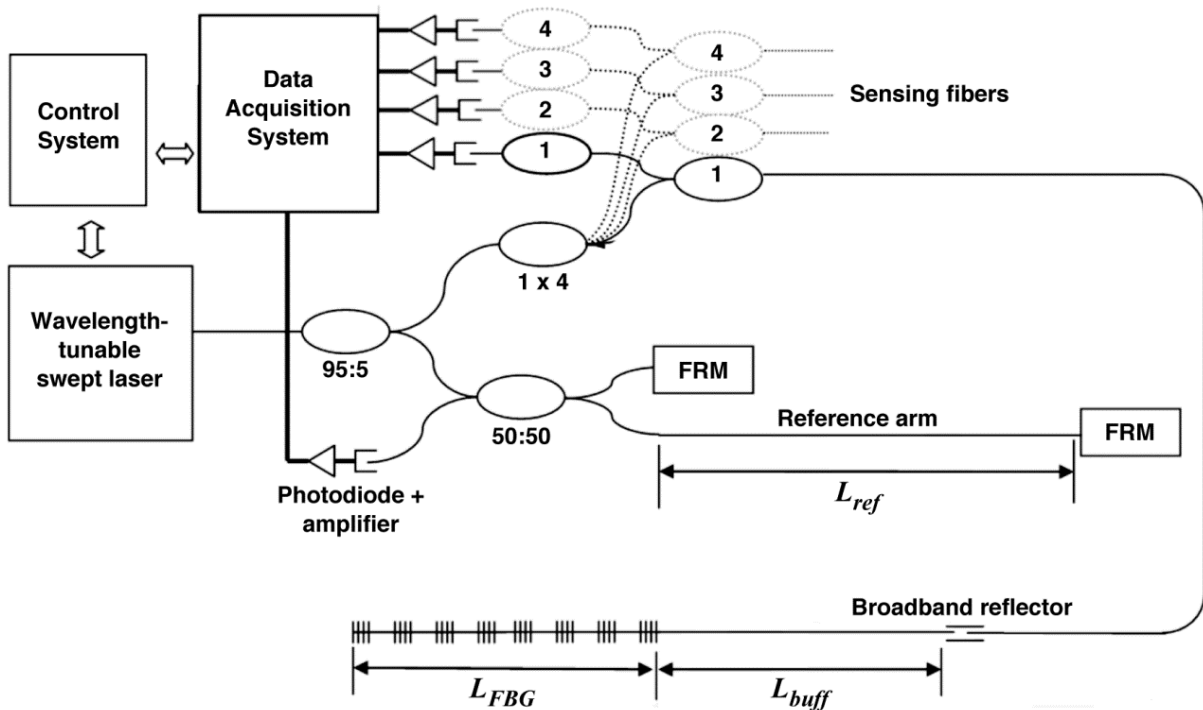


Figure 2-8: Fiber Optical Network with Reference Arm.

Applying Fourier transform to the intensity information gathered from the wavelength sweep range, this information is then mapped from wavelength domain to spatial domain (Figure 2-9). From the spatial domain each corresponding reflection represents each grating at its unique distance. Since applied strain detected from each FBG is linear to its shift in resonant wavelength, each grating's wavelength can be determined by taking the inverse Fourier transform from the spatial domain back to the wavelength domain, where the resonant wavelength change can be monitored (Figure 2-10).

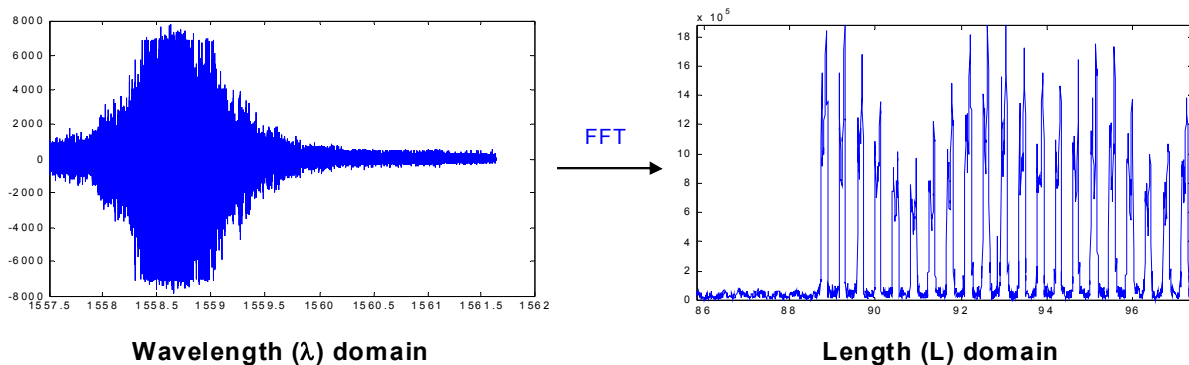
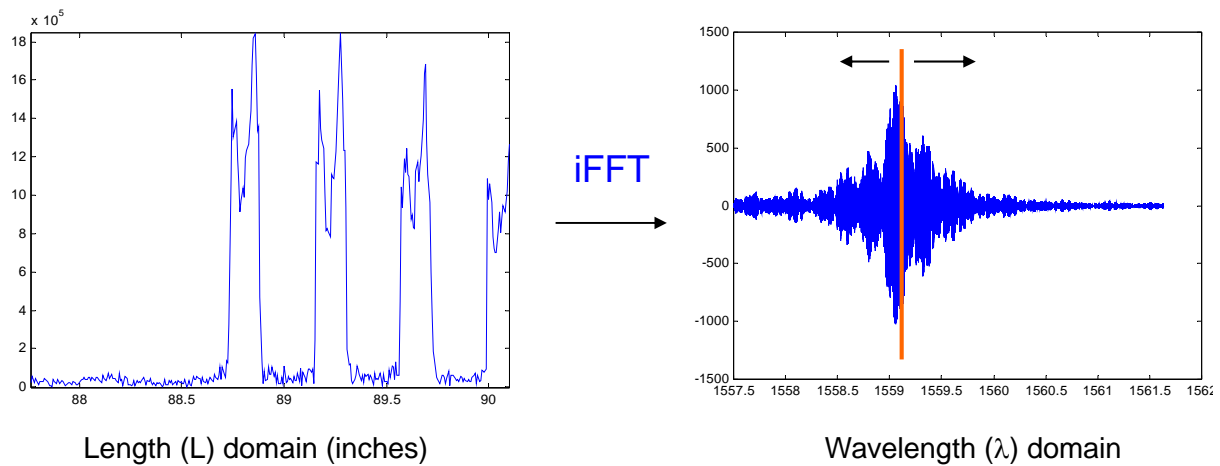


Figure 2-9: Fourier Transform from Wavelength to Spatial Domain to Discern Between Gratings.

## BACKGROUND



**Figure 2-10: Window Function and Inverse Fourier Transform from Spatial to Wavelength Domain.**

Applying this algorithm to real-time applications, where sample rates greater than five samples per second (sps) are needed, has proven to be limiting as a result of the initial Fourier transform. For applications requiring faster acquisition times, NASA Dryden has developed a method that yields acquisition speeds in excess of 60 sps. Recent advances in processing schemes, both in hardware and software have increased the sample rates of these systems to greater than 100 sps.

## Chapter 3 – SYSTEM DEVELOPMENT

### 3.1 GROUND-BASED INTERROGATION SYSTEMS

A system for interrogating FBG sensors has been designed and implemented for both ground and flight data acquisition applications. It has been designed to operate based upon a method first developed at NASA Langley (Hampton, Virginia) using OFDR to interrogate multiple Bragg gratings multiplexed onto a single fiber. [12, 13] This unique method allows for hundreds of Bragg sensors, spaced 1/2 in apart, to be located on a single fiber. NASA Dryden has taken this technology, which existed only in the laboratory, and has developed practical systems featuring compact size, robustness, and increased sample rates.

Ground-based systems (Figure 3-1) were developed initially to process fibers attached to sub-component specimens tested within the Flight Loads Lab (FLL) located at NASA Dryden; specimens such as composite and metallic panels, composite tubes, pressure vessels, a sub-scale simulated heat shield and the like. Several laboratory generations of the system have yielded a relatively small, quick, multi-fiber design that has been migrated to a flyable version.



Figure 3-1: Ground-Based 4-Fiber Interrogation System.

### 3.2 FLIGHT-BASED INTERROGATION SYSTEMS

The flight version of the system has been designed to operate aboard NASA Dryden's Ikhana aircraft, which is a modified General Atomics Predator B (Figure 3-2). This system performs much the same way as the ground version, featuring similar performance specifications while operating within the flight conditions of this aircraft; which include vibration, low temperatures, and elevated altitudes.



**NASA Photo ED07-0240-08**



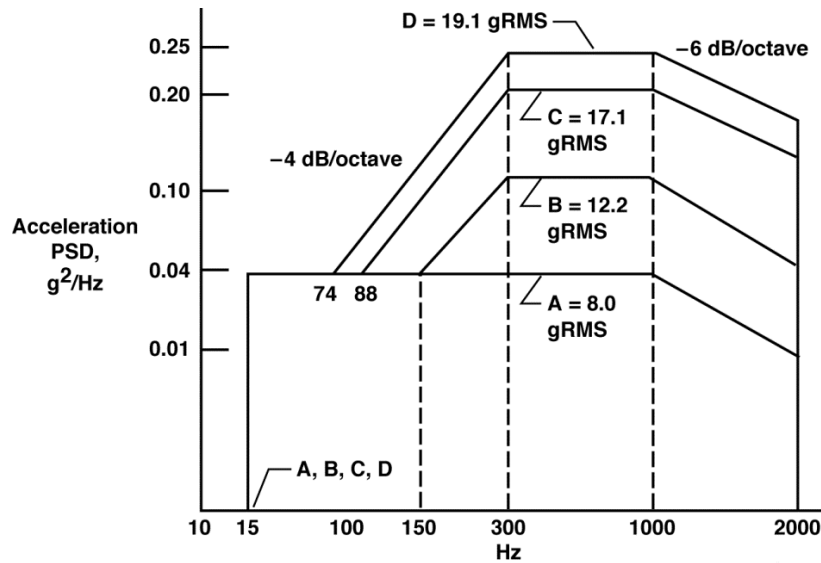
**NASA Photo ED07-0038-045**

**Figure 3-2: Flight 4-Fiber Interrogation System and Predator B Aircraft.**

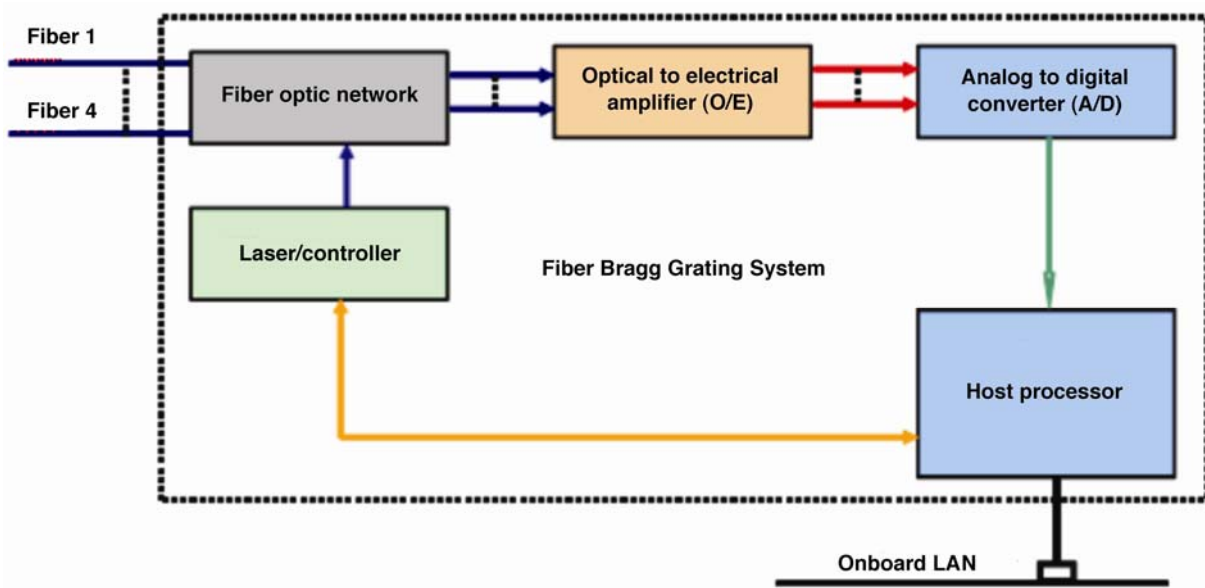
Throughout the remainder of this section, reference to “the system” will refer specifically to the flight system unless called out otherwise. The components, discussed later, of both systems are identical with the exception of the system enclosure. The flight system has a uniquely designed flight enclosure to satisfy system component environmental specifications while operating within the Ikhana aircraft. The ground-based system utilizes a Commercial-Off-The-Shelf (COTS) compact Peripheral Component Interconnect (cPCI) enclosure.

Designing a flyable version of the ground system was considered when an opportunity surfaced on-board NASA Dryden’s Predator B aircraft. The requirements of such a flight system would start with the measurement of strain distribution along the leading and trailing edge of the 60 ft wing span. Other requirements included a sample rate of 20 sps, +/-3500 microstrain, strain range, 4 fiber channels, 20 ft fiber sensing length, 30 lb maximum weight, 28 Vdc operation, and Ethernet interface. The environmental requirements were to meet NASA’s Curve A for sine wave vibration, -60°F to +110°F operating temperature range, and altitude of 60 K ft (Figure 3-3a).

The sub-components that make up the system are as follows: c-band tunable laser, optical network, Optical-to-Electrical (O/E) amplifier/converter, high speed Analog-to-Digital (A/D) converter, and host CPU with large mass storage capacity (Figure 3-3b).



a) Curve-A Random Vibration Standard.



b) System Block Diagram.

Figure 3-3: Environmental Qualification Requirements and System Design for the Ikhana Flight System.

The tunable laser is a COTS available, swept class-C laser capable of greater than +8 dBm output power and sweeps over a 30 nm range at speeds of up to 2000 nm/s. The laser can be used to interrogate lengths up to 328 ft, which is its coherence length. The unit resides on the cPCI bus and is configured, controlled, and monitored via the host cPCI processor.

The optical network and the O/E amplifier were designed to interrogate 4 sensor fibers each capable of sensing approximately 20 ft of 1/2 in spaced Bragg gratings, yielding 480 gratings per fiber or 1920 gratings per system. The O/E amplifier module combines negatively biased photodiodes with transimpedance

## SYSTEM DEVELOPMENT

---

amplifiers generating an electrical signal representative of the reflections from the Bragg gratings. The four amplified electrical signals are sampled by a 25 MHz, 4-channel 12-bit A/D cPCI card then buffered into the host CPU for data processing.

The host processor is an Intel-based Core Duo processor running at 2.1 GHz. The processor provides control and management to the tunable laser and data acquisition control for digitized data from the A/D. The processor also provides data processing and storage capability as well as data broadcast via the Ethernet connection.

The processing software, which implements the Dryden method mentioned earlier, can be configured to operate in 2 or 4 fiber mode. In the 4-fiber mode, the system can achieve sample rates of 30 sps, and while in its 2-fiber mode, 60 sps. The software can be configured to operate stand-alone or be controlled by a remote computer via the Ethernet connection. The system components were assembled within a 3/4 ATR flight enclosure powered from 28 Vdc aircraft power. The final flight system had dimensions of 7.5 in. by 13 in. by 13 in. and weighted 23 lb as shown in Figure 3-2.

As mentioned earlier, environmental testing was performed to qualify it to operate on-board Ikhana. The system was subjected to multiple 8 g shocks and sinusoidal vibration of 1.1 g peak up to 500 Hz. Elevated altitude testing of 60 K ft in conjunction with -60°F temperatures as well as elevated temperatures of 110°F to simulate the aircraft stationary on the tarmac, operating.

## **Chapter 4 – SENSOR CHARACTERIZATION AND ATTACHMENT**

Prior to the collection of any practical strain measurement, an investigation must be undertaken to develop and evaluate the attachment techniques used to bond the sensor to the requisite substrate. Early attempts at bonding surface-mounted fiber optics sensors to structural surfaces began with a logical extension of strain gage attachment methods developed over the past four or five decades. Past experience at Dryden with strain gage attachment up to 2000°F was used as a general guide for the accurate characterization and reliable attachment of FBG sensors. For high temperature applications, such as for aerodynamic and combustion heated structures, initial attachment studies were conducted on monolithic titanium to minimize the measurement uncertainty associated with an uncharacterized sensor with a complex material substrate. Several different combinations of strain gage epoxy adhesives have been tested and evaluated with fiber optic strain sensors. After several iterations, good agreement with conventional strain gages was obtained at room temperature, 350°F, and 550°F. Additional studies on surface attachment and characterization of fiber optic sensors are referenced. [14-18]

### **4.1 FBG TRANSVERSE SENSITIVITY**

Similar to conventional strain gages, FBGs are considered to be intrinsic sensors, that is, the physical transduction takes place within the medium itself. Conversely with extrinsic sensors, the measurement takes place outside the sensing medium, most commonly in air (e.g. the Extrinsic Fabry Perot Interferometer, or EFPI). For foil strain gages, the strain gage resistive element experiences a change in resistance due to the strains produced in the structure to which the element is attached. Similarly, the Bragg grating sensor experiences a change in wavelength due to strains that are transferred from the straining structure to the FBG sensor. The implication of intrinsic measurements is that they possess an undesirable sensitivity to transverse strains and temperature effects.

Ideally a strain sensor is only sensitive to strains along its primary axis and completely insensitive to strains in all other directions. For this reason, the resistive strain gage has been designed to maximize sensitivity to axial strains while minimizing sensitivity to transverse strains by geometrically increasing the area of the end loops in its resistive grid, as described by a strain gage manufacturer. [15] Even with these attempts at minimizing the error, the strain gage sensitivity to transverse strains is usually not zero. However, the transverse sensitivity for both strain gages and FBGs is a systematic error and can be successfully eliminated.

### **4.2 FBG TEMPERATURE SENSITIVITY**

For conventional strain gages, temperature sensitivity is a non-trivial problem resulting in the publishing of literally volumes of studies over the last 50 years to help cope with this phenomenon. These studies are well beyond the scope of this present work – some are referenced, see [16]-18]. Although the methods developed for conventional strain gages are by now well established and tractable, the temperature sensitivity issue nevertheless represents an added complexity that must be dealt with to ensure that accurate strain data are acquired.

Mechanical strain measured in a varying temperature environment can be corrected for temperature by accounting for apparent strain, similarly as to what is done when using a single active foil strain gage. Apparent strain is the strain component contributed to the expansion of the substrate material and the thermal output of the FBG sensor itself (eq. (1)). The apparent strain correction curve is generated by bonding the FBG strain sensors to an exact substrate material sample and heating slowly to the maximum

## SENSOR CHARACTERIZATION AND ATTACHMENT

test temperature (avoiding thermal stresses). The generated curve is then subtracted from indicated strains as a function of temperature to derive applied true strain or thermal strains for stress analysis (eq. (2)).

$$\varepsilon_{\text{app}} = (\alpha_{\text{sub}} + \xi)\delta T \quad (1)$$

$$\varepsilon_{\text{true}} = \varepsilon_{\text{ind}} - \varepsilon_{\text{app}} \quad (2)$$

In general, FBGs are sensitive to both temperature and strain effects simultaneously. Therefore to make accurate temperature measurements with FBGs, the strain response from the structure must be separated from the temperature response. FBG strain sensitivity is eliminated from the FBG measurement by encasing the grating in a small tube and bonding the tube, usually made from polyimide, to the structure. The tube effectively decouples the FBG from the structural strain and is therefore only sensitive to the temperature environment. If the FBG tube is small and the thermal environment is sufficiently uniform, the temperature difference between the bonded tube encasing the FBG and the substrate is usually negligible. The resulting indicated output from the encapsulated FBG that is produced by thermal loading is converted to engineering units of temperature using strain/temperature calibrated curves that are generated in the laboratory.

Figure 4-1 illustrates the typical installation for measuring strain and temperature with both conventional and fiber optic sensors. The figure shows a standard installation of a conventional strain gage, a conventional spot-welded thermocouple, an FBG strain sensor, and an FBG temperature sensor (in a polyimide tube).

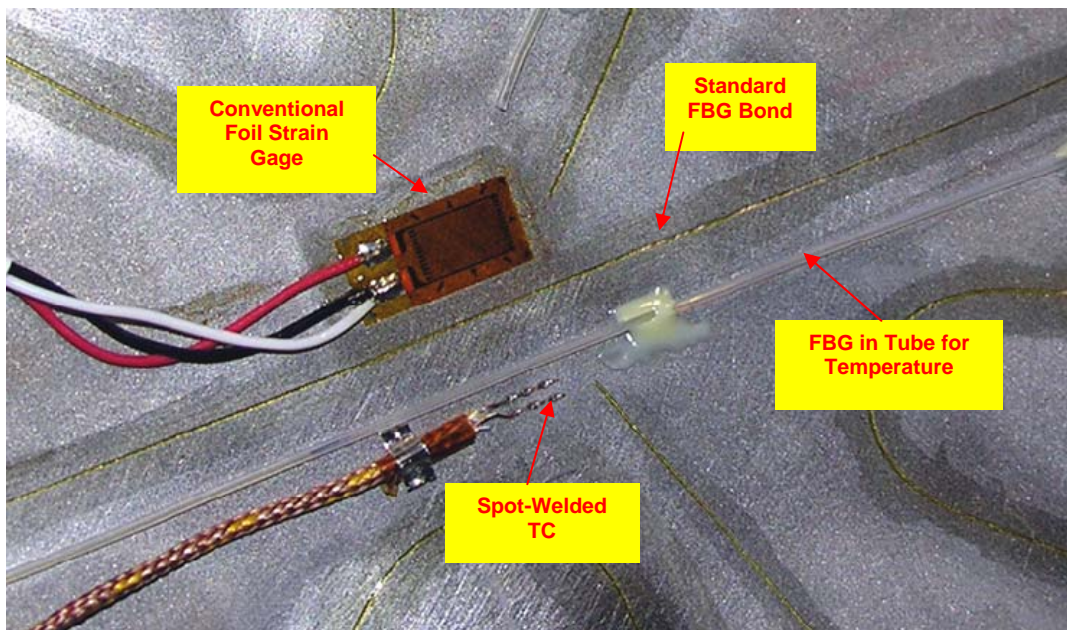
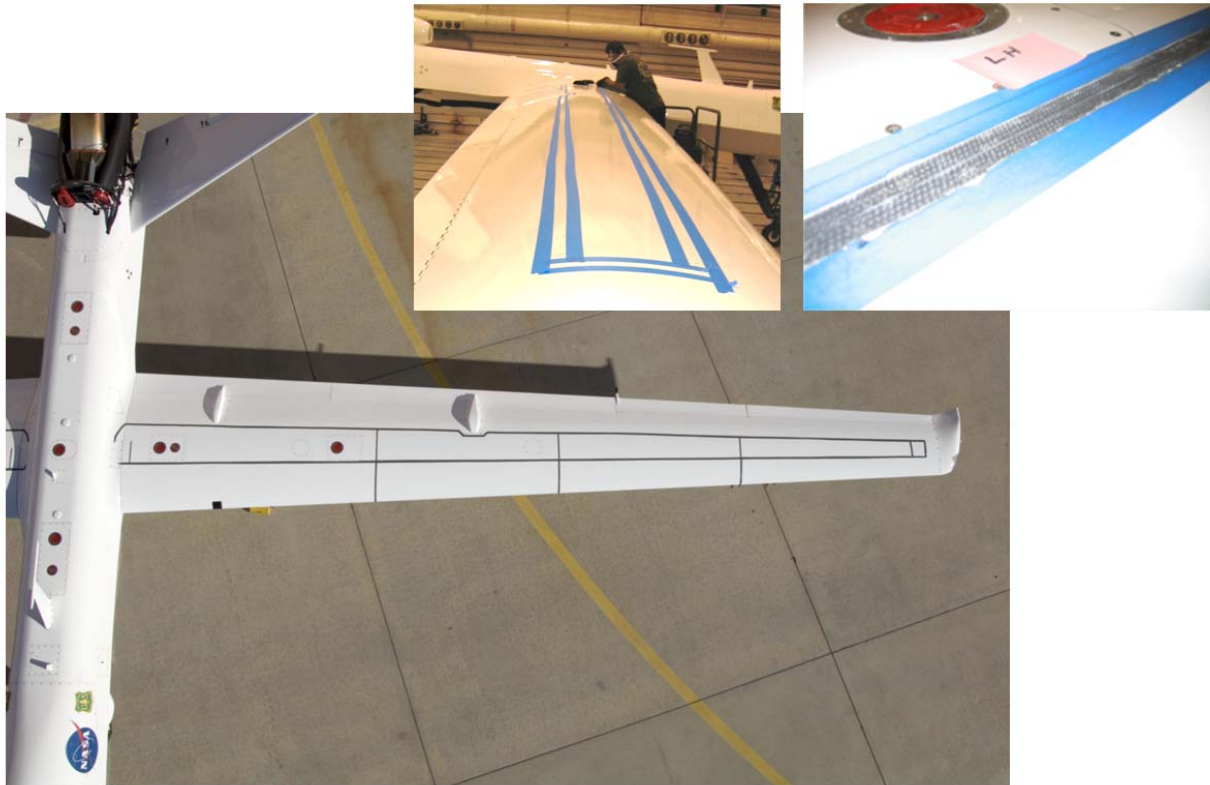


**Figure 4-1: Typical Installation for Measuring Strain and Temperature.**

Past work at NASA Dryden has included the installation of approximately 3,000 FBG strain sensors located on six 20-ft optical fibers bonded to the upper wing surfaces of an existing Predator-B, named Ikhana (Figure 4-2). These fibers were installed using conventional foil strain gage installation techniques. Such conventional installation methods involved the masking of approximately 120-ft-long by 3/4 in-wide runs on the upper wing surfaces, hand grinding the paint and filler down to the composite wing surface along these runs, adhering the optical fibers to the surfaces using conventional foil strain gage adhesives and procedures, sealing/aero-fare with class B-1/2 polysulfide polymer compound over the installation,



and re-painting. Though this method was successful for the entire flight test program, it was obvious more efficient installation methods would greatly enhance the practicality of covering large fuselage acreage or long wing spans.



**NASA Photo ED07-0287-08**

**Figure 4-2: Installation of FBG Fiber on Wing Upper Surface of Dryden's Predator-B UAV.**

To support future requirements for installing copious numbers of sensors in geometrically challenging sensor arrays, new paradigms for sensor characterization and attachment are required. NASA Dryden has been pursuing more efficient techniques for large-scale application of large number of sensors on the aircraft surfaces. One promising technique involves combining these FBG networks into an integrated structural health-monitoring package for installations on large-scale aerospace vehicle structures. As a first step in achieving this overall goal, an integrated demonstration was initiated in which FBG strain sensors for usage monitoring was integrated into a single package that significantly simplified current attachment techniques for large-scale application. These first steps have been directed at measurement validation and addressing a deficiency in bonding enormous number of fiber optic sensors to the surfaces of realistic structures using conventional methods. Highlighted here are past methods used to apply fiber, and the work being done to make the method of installing dense forms of instrumentation on aircraft more efficient.

### **4.3 ADVANCED SURFACE-MOUNTED INSTALLATION METHODS**

As the next step towards the high-level goal of more efficient integrated installations, NASA Dryden partnered with Acellent Technologies, Inc. (Sunnyvale, California) to develop innovative concepts and approaches for the attachment of thousands of fiber optic sensors. These sensors were multiplexed along dozens of optical fibers, arrayed in complex patterns (to accommodate rosette measurements) and bonded to the surface of complex aerospace vehicle structures (e.g. lifting surfaces, fuselage, bulkheads). Initial work

involved incorporating Acellent’s patented SMART Layer technology with FBG strain sensors and validating strain and temperature measurements embedded in the polyimide layer or sheet. Side-by-side fibers bonded using conventional methods, as on the Ikhana experiment, and fiber embedded in the SMART Layer were compared (Figure 4-3). Combined thermal/mechanical cantilever bending tests confirmed no undesired effects were induced by the polyimide layer and no effect to sensitivity, or gage factor, of the gratings were detected in both tension and compression, and at room temperature or elevated temperatures of 300°F. [19] These SMART Layer sheets could now be upsized and attempts to co-bond the layer during manufacture processes were initiated for larger scale test articles and aircraft wing or panel applications.

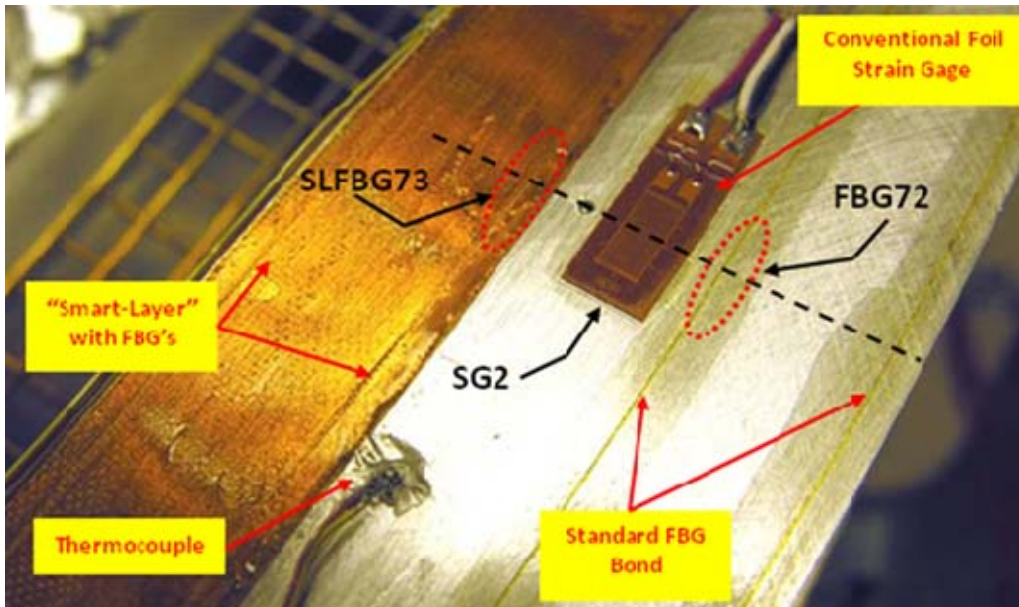


**Figure 4-3: Typical Collocated Cross-Section with Conventionally Bonded FBG, Conventional Foil Strain Gage, and FBG Incorporated into the SMART Layer.**

Given that the SMART Layer had negligible effect on the measurement compared to conventional direct bonds on the coupon level, the next goal was to address the applicability of the SMART layer for large-scale realistic aircraft structures. Such structures have added complexity due to complicated geometries, numerous egress ports for umbilical attachments, communications and power connections, fuel tank ports, actuator housings, and structurally complex features such as stiffeners, flanges, gaps, and wing folds. These geometric complexities make the extension of conventional approaches, such as those used on the Ikhana flight experiment, for realistic aerospace structures especially difficult.

**4.4 ADVANCED EMBEDDED INSTALLATION METHODS**

Work has begun with composite manufacturers in co-bonding the SMART Layer during the fabrication process. It is believed this method of a co-bonded surface installation will avoid typical problems encountered when embedding the fiber at depth into the composite material itself. As mentioned earlier, embedded FBG strain sensors are sensitive to transverse strain, which occur during tensile or compressive loading. In addition, if the fiber is embedded, bending strain outputs would be reduced as a function of distance from the neutral axis. Bonding on or near the surface of the structure not only eliminates these undesired traits, but the polyimide SMART Layer will also provide added protection from incidental damage.

Overall, the SMART Layer has potential to help transform installation methods for future aircraft sensor installations.

## **Chapter 5 – ON-BOARD STRUCTURAL TRANSFER FUNCTIONS**

One of the most significant benefits of FOSS technologies and FBG-OFDR is the amenability for these measurements to be used in conjunction with closed-form analytical equations. These so called data-driven models, can use a multitude of highly multiplexed FBG measurements to accurately determine a variety of engineering parameters in real time. Parameters such as wing shape, structural properties, externally applied aerodynamic forces, mode-shapes, and fatigue life have proven very difficult to determine, especially in real-time flight environment. Because these transfer functions are analytically- and not numerically based, they provide exact solutions to partial differential equations and are therefore very accurate. This accuracy is further ensured because the models are continuously updated in real time with the structure's physical response during flight. Furthermore, this approach is more amenable to real-time on-board processing because these equations can be fed with actual in-flight data efficiently as compared to numerical methods, such as finite-element models. Numerical finite-element approaches, which usually consist of thousands of degrees of freedom and the mathematical inversion of large stiffness matrices, have proven too cumbersome for real-time implementation. This section presents three of these data-driven on-board structural transfer functions: wing shape, external loads, and fatigue life.

### **5.1 WING SHAPE**

Wing shape transfer functions based on NASA Dryden patented technology [20] have been developed, implemented, and flight validated. Two of these displacement methods are presented in the following section.

#### **5.1.1 NASA Dryden Real-Time Data-Driven Displacement Methods**

Development of data-driven displacement methods for determining the deformed shape of structures was motivated in 2003 by the Helios flying wing, which had a 247-ft wing span with wingtip deflections reaching 40 ft (Figure 5-1). The Helios flying wing (AeroVironment Inc., Monrovia, California) failed in midair in June 2003 due to possible un-damped pitch oscillations of highly deformed wing. The Helios mishap created the need to develop a new technology to determine in-flight deformed shapes of unmanned aircraft wings and then visually display the results to ground-based pilots to ensure flight safety.



**NASA Photo ED01-0209-2**

**Figure 5-1: Helios UAV (AeroVironment Inc.).**

Using a data-driven modeling approach, the structure deformed shape could be determined by feeding the surface strains into real-time structural transfer functions for transforming the surface strains into out-of-plane deflections and cross-sectional rotations for mapping out the overall deformed shapes of the structure. [6, 21-23]

FBG-OFDR fiber optic strain sensors are the most attractive candidate to accurately and comprehensively determine structural shape and are the most practical approach to input into the structural transfer functions. The highly multiplexed sensor output is input at strain-sensing stations at desired sensing intervals. The conventional strain gage system is impractical for flight vehicles because of excessive lead wire weight. Another powerful characteristic of FBG-OFDR is that the strain-sensing station number can be increased easily as needed using a single command without the need to actually install additional strain sensors one by one as in the case of conventional strain gage system.

**5.1.1.1 Theory**

Displacement equations combined with the on-board fiber optic strain-sensing system form a new powerful tool for in-flight deformed shape monitoring of flexible wings and tails, such as those often employed on unmanned flight vehicles by the ground-based pilot for maintaining safe flights. In addition, the real-time wing shape monitor could then be input to the aircraft control system for aero-elastic wing shape control.

**5.1.1.2 Formulation**

The formulation of the displacement transfer functions stemmed from the integrations of the beam curvature equation (second order differential equation). An aircraft wing, considered as a cantilevered beam-like structure was first discretized into multiple small domains so that beam depth and surface strain distributions could be represented with piece-wise linear functions. This discretization approach enabled stepwise integrations of the beam curvature equation in closed forms to yield slope and deflection equations for each

domain in recursive formats. The final deflection equations in summation forms (called displacement transfer functions), which contain no structural properties (such as bending stiffness), were then expressed in terms of domain length, beam depth factor, and surface bending strains at the domain junctures. In fact, the effect of the structural properties is contained in the surface strains.

**5.1.1.3 Implementation**

For flying wings, such as the Helios-class UAVs, the two-line strain-sensing system (Figure 5-2) is a powerful method for simultaneously monitoring the bending and cross-sectional rotations. [23] The two-line strain-sensing system eliminates the need for installing the shear strain sensors to measure the surface distortions through which the wing structure cross-sectional rotations could be determined.

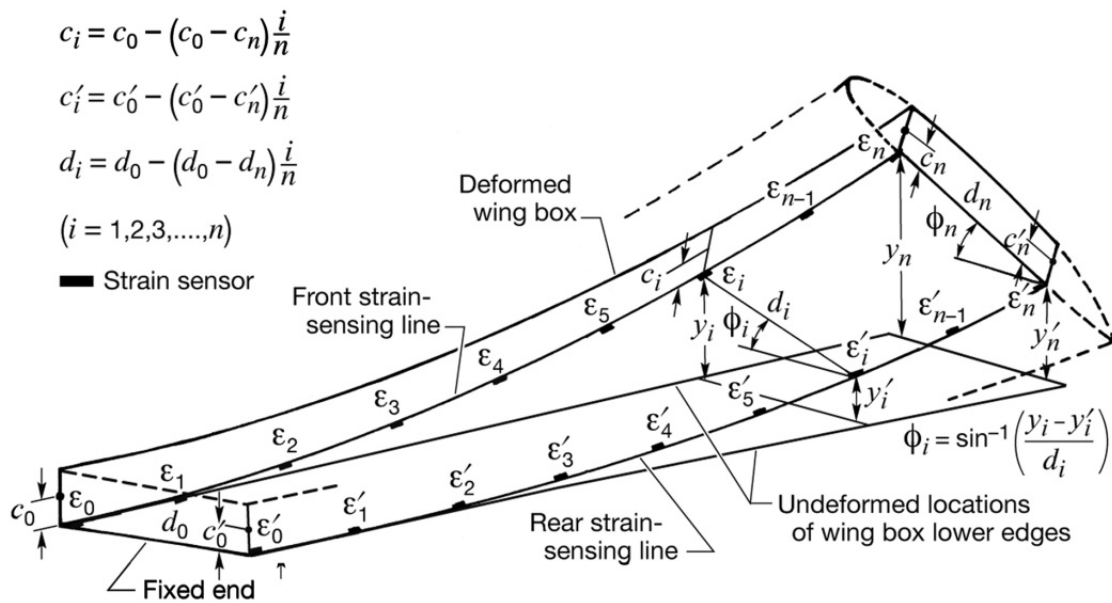


**Figure 5-2: Tapered Wing Box Instrumented with Two-Line Strain-Sensing System.**

By averaging the front and rear deflections calculated from the displacement transfer functions using the measured surface strains, torsion effect may be eliminated to yield the true bending deflections of the wing structure. Also, the calculated front and rear deflections can be used to calculate wing structure cross-sectional rotations due to torsion effect. Thus, the overall structure-deformed shapes can be mapped out for visual displays before the ground pilots, thereby accomplishing the objective of in-flight wing structure deformed shape sensing.

Recently, the NASA Dryden real-time displacement method was applied on a 175-ft span full-scale wing. [24] FBG-OFDR-acquired strain measurements were input to the displacement transfer functions. Wing tip displacements determined using the Dryden method were within +/- 2.7 in (out of 155-in max deflection) for nearly all the load steps, indicating that the fiber optic-based displacement method can be relied upon to accurately determine wing displacement on realistic structures using real-world measurements.

**5.1.2 NASA LaRC/Dryden Displacement Theory**

Although a very powerful tool, one of the drawbacks of the methods described above is the requirement to transfer structural strains from a substrate structure, such as the aircraft wing, to the FBG sensing element in order to calculate structural shape. Recent research has resulted in an alternative approach that can determine

wing shape without the requirement to first transfer surface strains from the structure into the surface-mounted FBG sensor. One of these developments is the fabrication of FBG sensors written inside a multi-core fiber. Typical FBG sensors are written into a regular communication-based single mode fiber, which has one narrow core (~8- $\mu\text{m}$ ) that resides in the middle of the optical waveguide surrounded by a cladding region. In a multi-core fiber, there are three individual cores; each core is 120 degrees apart (Figure 5-3a). Each core supports a particular single mode, therefore acting as if three single mode fibers are bundled together. By creating an algorithm that relates the cylindrical symmetry of the strain distribution, it is theoretically possible to recreate the shape of the sensors. However, there were limitations that existed to the technology. Multi-core fiber is considered to be a specialty fiber and therefore expensive. The multi-core fiber is also difficult to manufacture. Fusing a multiple cores into a conventional single mode fiber is challenging. Another aspect is that the prior-developed shape-sensing algorithm cannot recreate shape in real time.

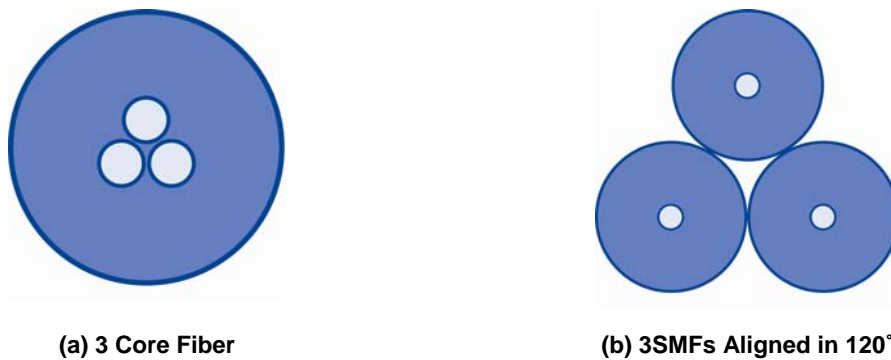


**Figure 5-3: Three-Core Fiber and Three Single-Mode Fibers Arranged 120° Apart.**

In recent years, NASA Langley has developed and patented a software algorithm that can distinguish shape with respect to strain based on the three-core fiber concept. [25] However, a limitation of the methods was that in order to demonstrate shape sensing, strain information of the smart-fiber first needed to be pre-determined and calculated to obtain the desired shape. To overcome this limitation for real-time operation, NASA Dryden collaborated and integrated NASA Langley’s software into the high-speed, real-time fiber grating interrogation system. A demonstration apparatus, which consists of a hexagon rod with 3 faces, 120 degrees apart instrumented with three individual FBG sensors, is fabricated and demonstrated with Langley’s algorithm. Results show shape sensing is possible and accurate for the bending of structures in all directions. Knowing the strain value of each fiber, the three-dimensional position of the fiber can be accurately rendered in real time.

The advantage of the three-core shape sensing is that it provides additional installation flexibility. Three fibers can be bonded together as shown in Figure 5-3b, or they can be attached 120 degrees apart on a very flexible structure, like a hose or cable. There is no requirement for the fiber to be mounted on a structural component in order to calculate structural displacement. In addition, the derivative of the deforming structure does not have to be unique (i.e. there can be hinges, wing folds, et cetera). The fiber shape can be determined from the fiber deformation alone, without requiring a carrier structure to transfer strain to the FBG sensors.

The three single-mode fiber approach has opened up new applications for aerospace vehicle monitoring and control. Other sectors of society have benefited as well, such as the medical community. NASA Dryden collaborated with a medical company to physically bundle three single-mode-fibers with FBGs, where FBG sensors are spaced 1/2 in apart, into one single-fiber structure with a total diameter >300  $\mu\text{m}$ . By utilizing the same algorithm, the shape of this smart-sensor can be accurately recreated from the strain information. There are many potential applications to this shape sensing technology, from large-scale

aerospace applications such as wing-shape monitoring all the way to medical applications such as integration within robotically controlled cardio-catheters.

## **5.2 STRUCTURAL PROPERTIES AND EXTERNAL LOADS**

In addition to wing and component shape, efficient real-time structural monitoring transfer functions have been developed to provide extensive information about the physical response of structures under load. [26] Similar to the previous examples, these transfer functions are driven by actual strain data to accurately measure local strains at multiple locations on the surface of a structure. Through a single point load calibration test, these structural strains are then used to calculate key physical properties of the structure at each measurement location. Such properties include the structures flexural rigidity (the product of the structures modulus of elasticity,  $E$ , and its moment of inertia,  $I$ ), and the section modulus (the moment of inertia,  $I$ , divided by the structures half-depth,  $c$ , or  $I/c$ ). The resulting structural properties at each location can be used to determine the structures bending moment, shear, and structural loads in real time while the structure is in service.

The amount of structural information can be maximized through the use of highly multiplexed FBG technology using OFDR. Since local strains are used as input to the transfer functions, this system serves multiple purposes of measuring strains and displacements, as well as determining structural bending moment, shear, and loads for assessing real-time structural health.

The method first requires that an aircraft wing, preferably instrumented with a high number of multiplexed FBG sensors, be subjected to a simple point-load calibration test for bending and torsion. Using the classical bending equation for a uniform beam, the structural properties of the wing structure can then be determined at a multitude of locations along the wing span. For the simple flexure case, the section properties can be determined by inputting the measured strains into equation (1).

$$(ES)_i = \frac{P(l - i\Delta l)}{\varepsilon_i} \quad (1)$$

These experimentally determined section properties from the as-built structure can be used for two purposes. The properties can be input in finite-element analysis because these properties are far more accurate than the properties normally assumed in finite-element models. These properties, together with measured in-flight strains can also be used to determine bending, shear, and external loads in real time during the flight. The external loads can then be used as feedback to adaptive control systems. Figure 5-4 shows an analytical demonstration of the method on a simple tapered wing, subjected to a distributed load along its span. The forces calculated from computationally-generated strains obtained from the method are shown in Figure 5-5.

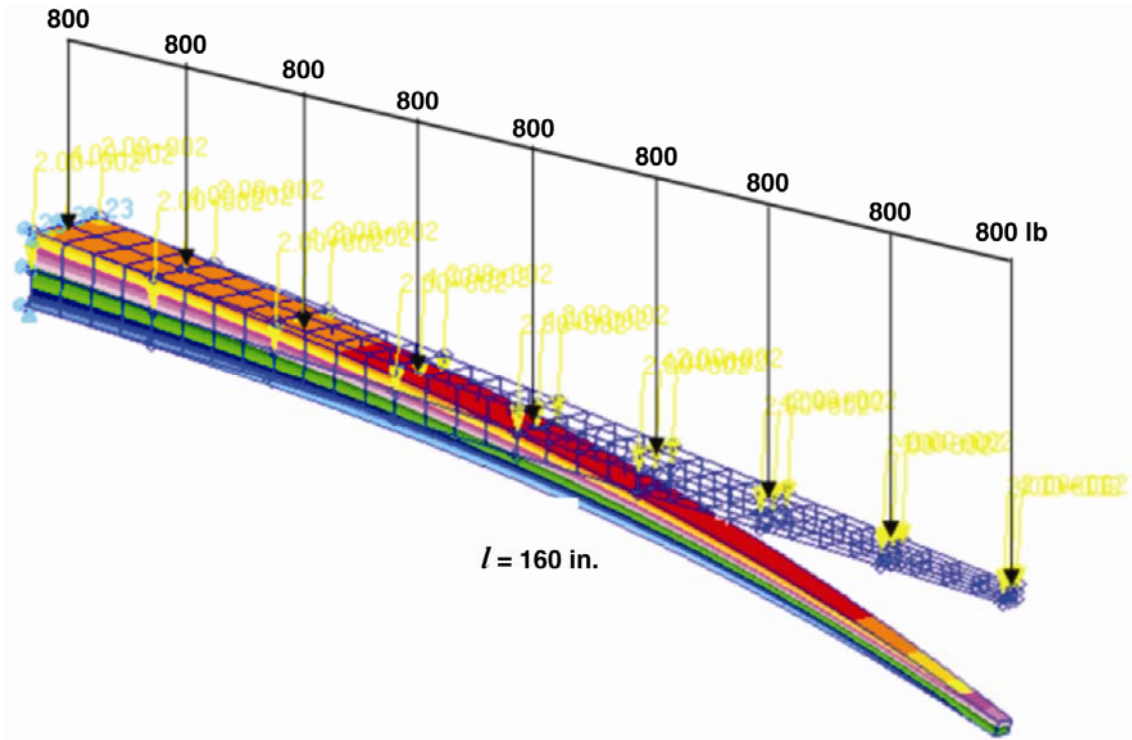


Figure 5-4: Finite-Element Model.

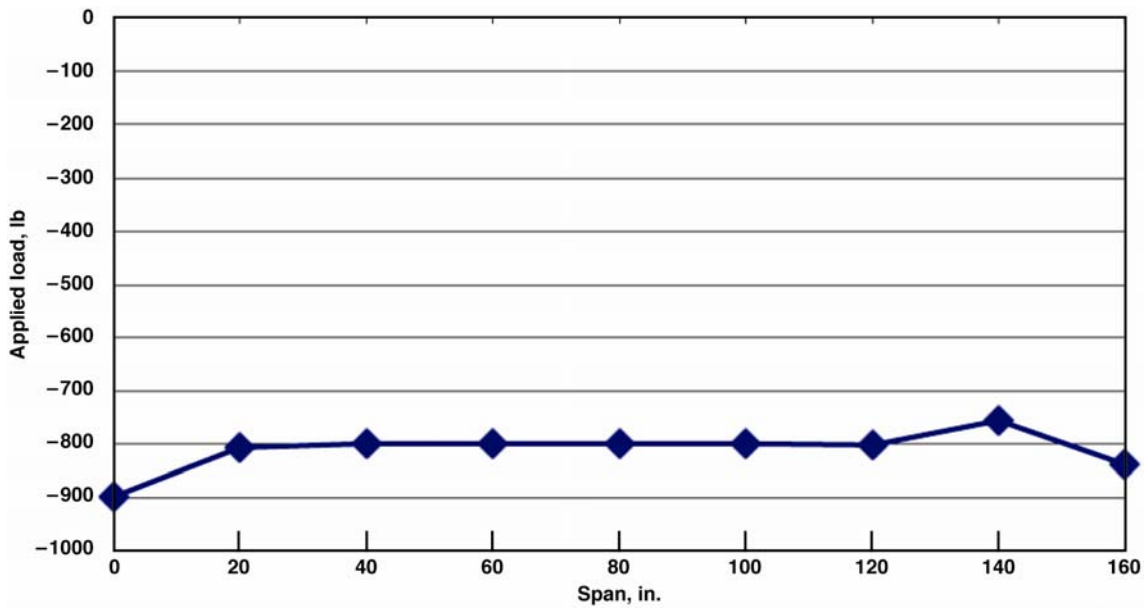


Figure 5-5: Analytically Determined Loads.

### 5.3 FATIGUE LIFE

For flight vehicles, most of the failure critical, high stress concentration points are located in hard-to-reach narrow regions where installments of conventional strain gages are practically impossible. FBG-OFDR



system technology is ideal for this application because FBG sensors possess high spatial resolution and can be conformed to fit the complex geometries in which critical stress points exist. The random stress cycles monitored by the fiber optic sensors can then be fed into the Walker crack growth equation to calculate the amount of crack growth induced by each flight. Based on the calculated crack growth, an operational life equation can calculate the remaining operational life (number of flights left) for each critical stress component. [27,28] A typical crack growth curve for B-52 pylon front hook (failure critical component) is shown in Figure 5-6.

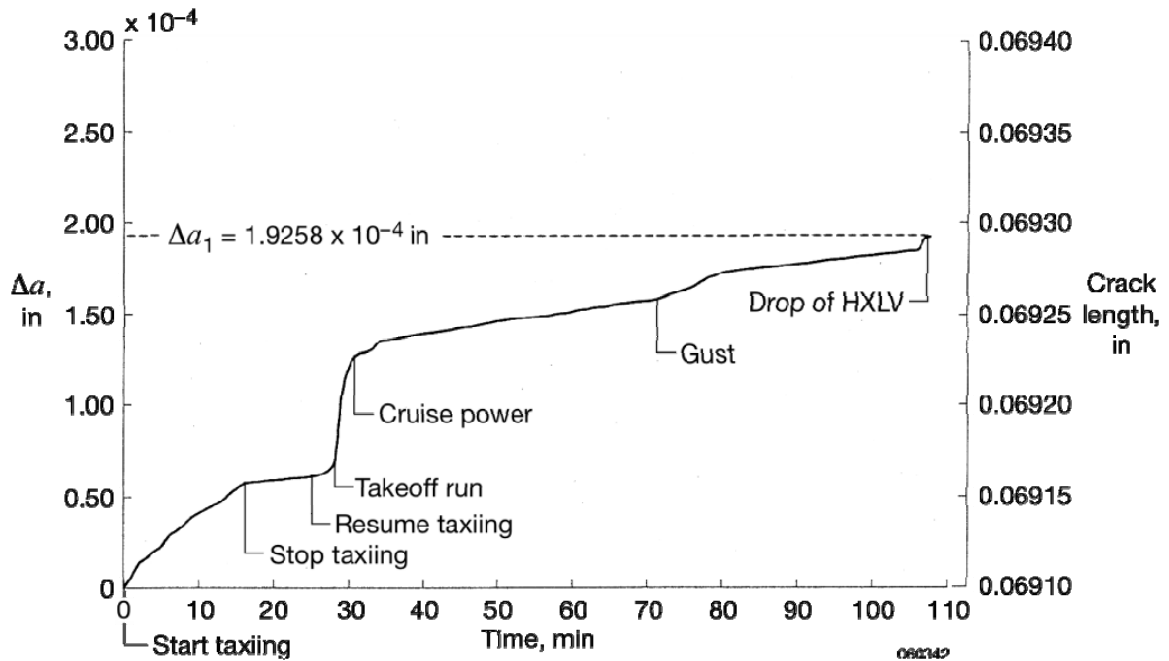


Figure 5-6: Typical Crack Growth Curve for B-52 Pylon Front Hook.



## Chapter 6 – RECENT EXAMPLES OF LARGE SCALE FOSS TESTING

### 6.1 NESC – COMPOSITE CREW MODULE STRUCTURAL TESTING

Dryden engineers successfully supported structural testing of the NASA Engineering Safety Center’s (NESC’s) full-scale Composite Crew Module (CCM) located at NASA Langley Research Center in 2009 – 2010. By deploying NASA-developed fiber optic sensors along the various windows, and docking port along the crew module; structural strains along these locations could be monitored in real time. Each optical fiber contained hundreds of strain sensors, where each sensor had a spatial resolution of 0.5 in and were sampled at least 20 times per second. The high spatial resolution of fiber optic sensors enabled strain mapping of geometrically complex regions throughout the CCM, where applying traditional strain gauges becomes difficult. These fiber optic strain sensors monitored repeatedly internal pressure loading test of the CCM in real time, with much faster strain-acquisition rate than commercially-available systems. Figure 6-1 shows the DFRC interrogation unit and regions (in red) where FBG sensors were located on the CCM test article. During structural testing, the crew module was subjected to internal pressure at up to 200% of design limit and under induced strain load to simulate conditions at space and re-entry via parachute deployment, respectively. Strain values observed from fiber optics sensors correlated well with finite-element predictions under different conditions, within 5% difference between predicted and measured values (Figure 6-2). The fiber sensors were also subjected to cyclic loads testing of the CCM and gave consistent readings, with no effect of material fatigue. At the end of the test program, the fiber optic sensors reliably measured strains during the ultimate CCM structure failure test, accurately recorded the time of failure, and observed the propagating shock wave as a result. Despite the high loads endured by the fiber sensors throughout testing, fiber optic sensing technology performed well and returned valuable data to assist in post-test data analysis.



**Figure 6-1: Ground-Based Four-Fiber Interrogation System and NESC CCM Testing.**

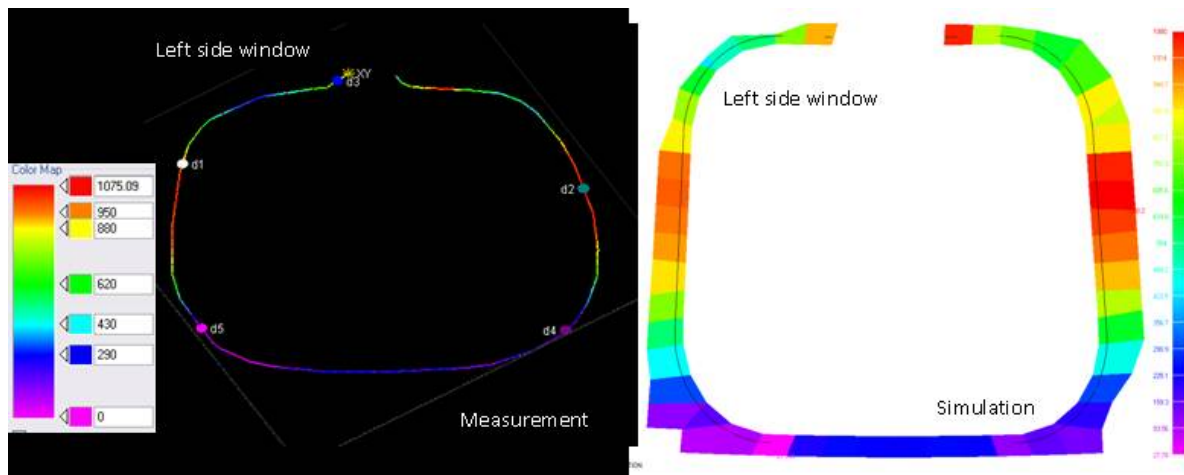


**Figure 6-2: Sample Real-Time Measurement Data (Left) of the Fiber Sensor versus Simulation Result (Right) of the Left-Side Window of the CCM During Maximum Internal Pressure Load.**

## 6.2 IKHANA

In June 2003, the Helios Prototype Unpiloted Aerial Vehicle (UAV) experienced significant pitch instability during low-altitude flight that led to a catastrophic structural failure and in-flight break-up. One of the most significant lessons learned from the mishap investigation was the need to provide real-time measurement of wing dihedral to the test crew during flight (Thomas Noll, et al, “Investigation of the Helios Prototype Aircraft Mishap Volume 1 Mishap Report”, NASA internal document, January 2004). A recent in-house study assessed the viability of using conventional strain gage instrumentation, and demonstrated that the wire weight alone represented a prohibitive weight penalty and was impractical to implement for many aerospace vehicles. Alternatively, lightweight and low profile fiber optic wing shape sensors in conjunction with computationally efficient transfer functions, were viewed as a promising approach to providing very accurate wing measurement calculations for eventual input to the flight control system for aero elastic motion control.

Flight validation testing was conducted at NASA Dryden in 2008 – 2009. Approximately 3000 FBGs were installed on the wings of NASA’s Ikhana vehicle (Predator-B) shown in Figure 6-3. The FBGs were used to sense the shape and monitor the stress of the Ikhana wings in real time throughout each mission. Determining wing shape in real time serves as the first step toward achieving the important goal of controlling the shape of subsonic fixed wing aircraft. The resulting capability also provided a practical approach to accomplish structural health and loads monitoring during the experiment. Research tasks were performed in the areas of algorithm development, system development, environmental qualification testing, system/vehicle integration, sensor installation, ground test validation, and experiment integration.



NASA Photo ED07-0287-03



NASA Photo ED07-0038-045

Figure 6-3: Ikhana UAV Vehicle with Sensors Installed (Left); in Flight Prior to Experiment (Right).

Research was accomplished toward the development and experimental validation of analytical strain-to-displacement transfer functions. [6] These transfer functions were developed to obtain both in-plane strain mapping and out-of-plane displacement measurements simultaneously for complex flexible structures, such as the wings of the Ikhana and many other subsonic fixed wing aircraft.

The NASA Dryden designed FBG-OFDR system was developed, environmentally qualified, and integrated in the avionics bay of the Ikhana vehicle, as depicted in Figure 6-4. This figure also shows the layout of sensors installed for the flight experiment.

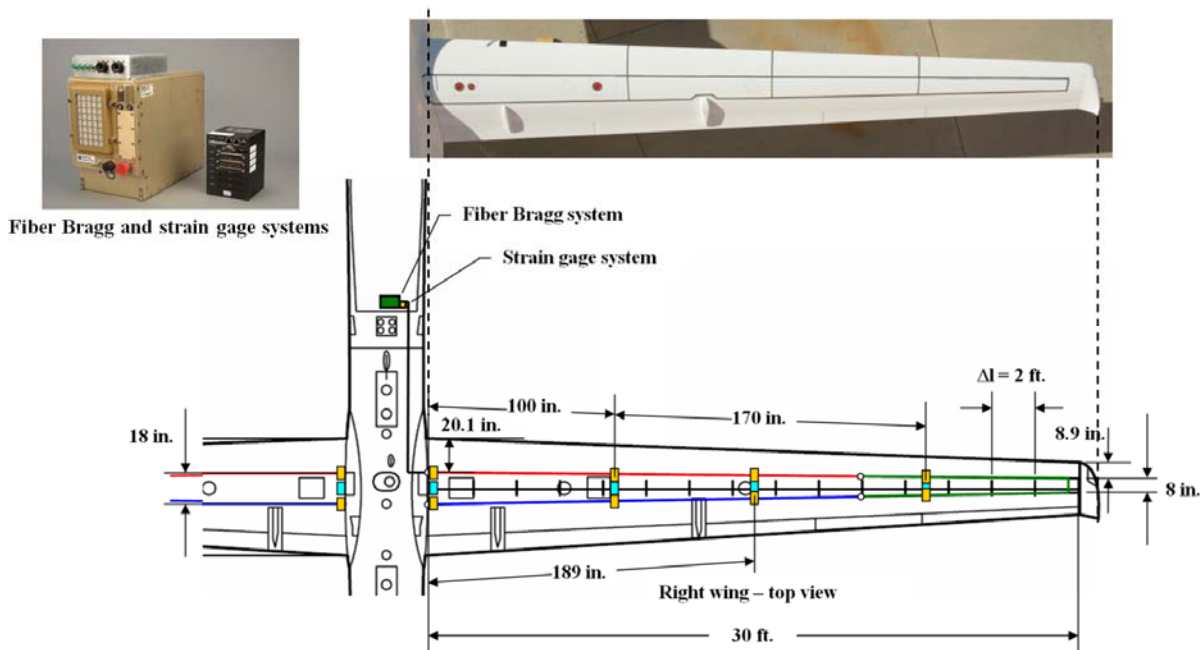


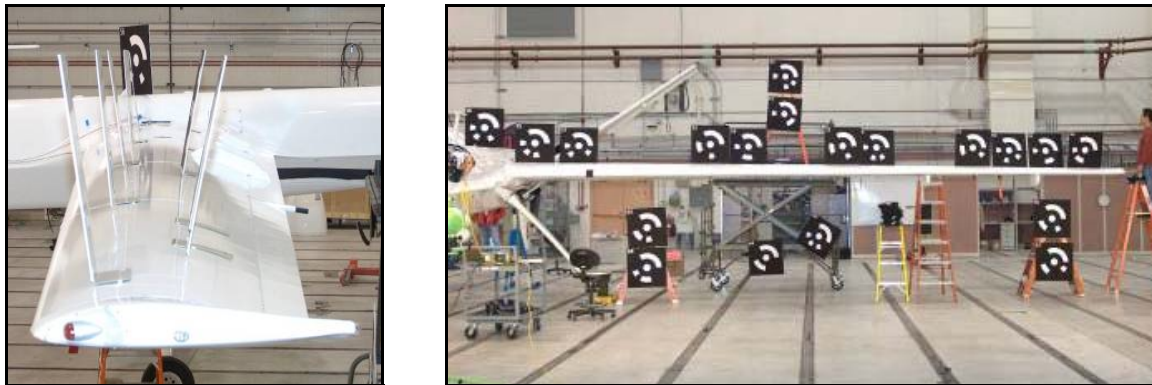
Figure 6-4: FBG Sensor Layout.

### 6.2.1 Sensor Attachment

In addition to approximately 3000 FBG strain sensors, 16 strain gages were used to validate FBG strain measurements. Eight conventional thermocouples were bonded to the upper wings of the vehicle and used primarily for strain sensor error correction as described in Chapter 4.

**6.2.2 Ground Testing**

Prior to flight testing, ground validation testing was conducted using Dryden’s high resolution/high speed optical measurement system as the validation standard (Figure 6-5). The optical system utilized bar-coded targets placed on the left wing and center fuselage at 10 measurement locations. Five load cases were applied through the use of calibrated shot bags as shown in the figure. The maximum loads applied to the wings were limited to 200 lb, which produced displacements at the wing tips of only approximately 3 in. Despite these small displacements, agreement between FBG and optical systems at the wing tip was 2.8% and 4.8% for the two bending load cases.



**NASA Photo ED08-0016-12**

**Figure 6-5: Ikhana Ground Testing.**

From May until August 2008, 18 flight tests totaling 36 flight-hours were conducted on the Ikhana vehicle. To our knowledge, these flight tests represented the first flight validation test of FBG strain and wing shape sensing. Figure 6-6 shows a screen capture of a control room display showing the data telemetered from the aircraft in real time. The figure shows a photo of the Ikhana vehicle (a modified Predator-B) with superimposed flight data. The yellow data are the 2000 FBG strain measurements from wing tip to wing tip with FBG measurements located every 10 mm. The measurements are in micro strain with the axis on the right. The strain values corresponding to the center fuselage on the airplane are not real, but are FBG sensors on the optical fiber spooled in the fuselage on unsupported regions. The red data are wing displacement measurements from wing tip to wing tip (with units on the left). These data and the trace at the bottom of the figure were produced during a “pitch up pitch down” maneuver. The pilot pushed down on the stick quickly, then quickly pulls up for several cycles. The bottom trace shows the deflection of the wing tips during the maneuver. Overall, the FBG system performed well throughout entire flight without any issues.

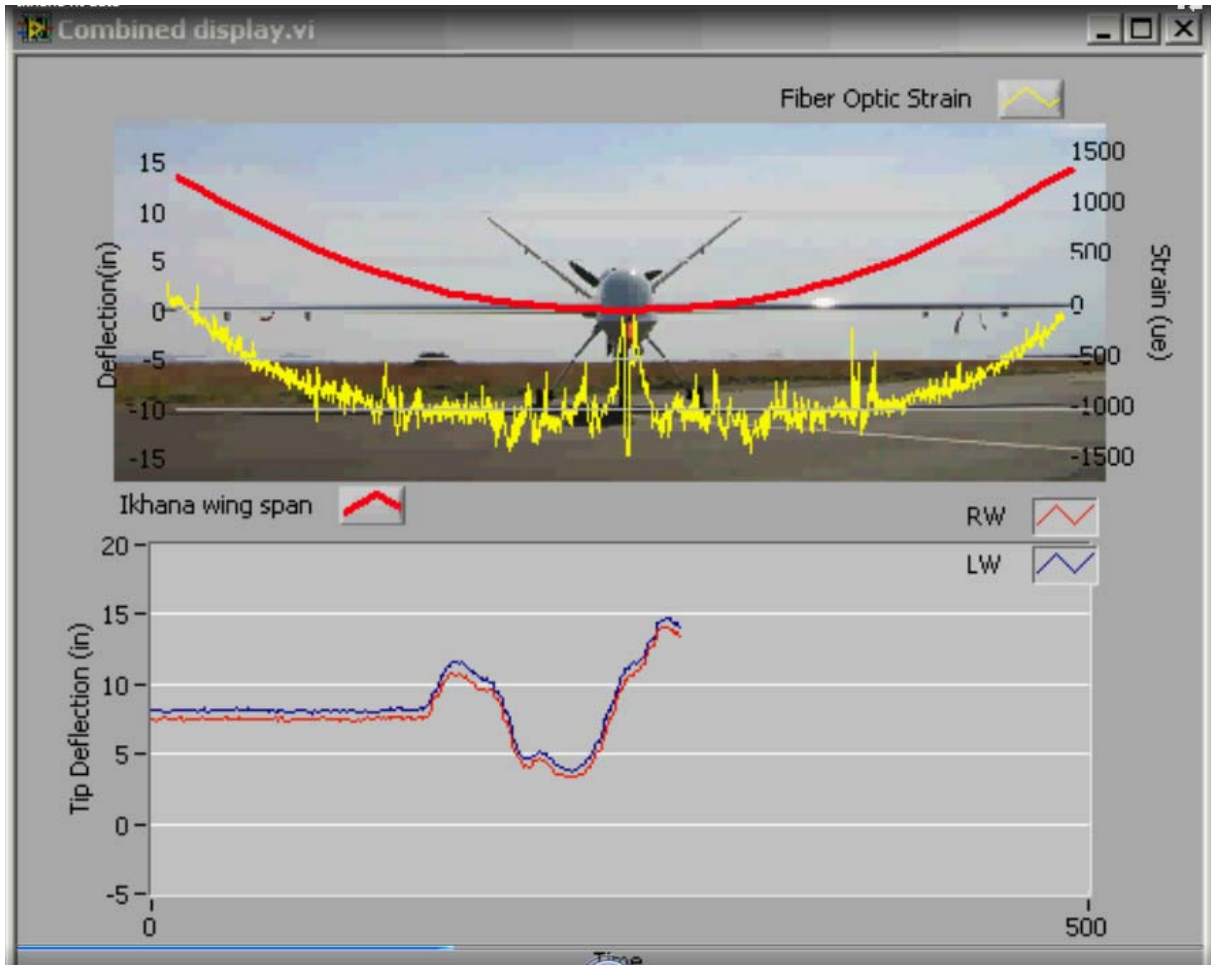


Figure 6-6: Ikhana Flight-Test Data.

## 6.3 GLOBAL OBSERVER

### 6.3.1 Flight Testing

Following the successful flight validation testing of FBG sensor technology on the Ikhana, NASA Dryden performed real-time strain sensing on AeroVironment’s Global Observer aircraft, a full-composite Unmanned Aircraft Vehicle (UAV) capable of stratospheric flight (up to 65,000 ft) at long intervals (over 7 days) without landing or refuelling (Figure 6-7). Optical fibers with highly multiplexed FBG sensors were installed throughout the left wing of the Global Observer for strain monitoring. In total, eight 40-ft long fibers were installed along the front and aft wing portions of the left wing, as well as one fiber that was installed on the fuselage of the aircraft to measure torsion of the fuselage. These eight fibers were written with over 8,000 FBG sensors in total. Strain information was recorded in real time through in-flight data acquisition system at 20 samples per second per sensor. Global Observer completed its maiden-flight on August 5<sup>th</sup>, 2010 with the FOSS system onboard and archiving data. The FOSS system has performed well, monitoring the strain distribution along the leading and trailing edges of the upper and lower surfaces of the aircraft’s left wing as well as on the aft fuselage, from take-off to mid-flight to landing. There were 5 subsequent test flights for the Global Observer, and the FOSS system successfully recorded the strain information for 4 of the 5 flights.



**Figure 6-7: Flight Interrogation Unit and the Global Observer UAV.**

### **6.3.2 Wing-Load Testing**

In addition to real-time flight testing, AeroViromen has partnered with NASA Dryden for wing-load testing of both wings of a future Global Observer, to be built after the current flight-testing of GO-1. These load tests occurred in July 2010 at NASA Dryden's Flight Loads Laboratory. The purpose of the wing-load test was to monitor the strain of the wing panels under load and to monitor the wing shape of the panels using the NASA-patented wing shape algorithm. Eighteen fibers, each consisting of up-to 1000 FBG sensors, were bonded to the forward and aft portion of both wings as well as to the fuselage. The ground-based fiber optic strain-sensing acquisition system is composed of three rack-mount units, where each individual unit is capable of measuring 8 fiber channels simultaneously at 50 Hz per sensor per fiber. The data from each system was then broadcasted to a server where all the data were recorded and displayed in real time. If more than 24 channels were needed, acquisition units were easily added for more robust measurements. In summary, the wing-load test composed of subjecting each wing panel to 100% of design load in both positive load and negative load at various angles of attack. Structural response of the wings was successfully quantified in the FBG-OFDR, photogrammetry, and traditional strain-gauge systems at various locations. Post-data analysis verified that the FOSS measurement is in agreement with traditional strain gages. [24]



## **Chapter 7 – THE FUTURE OF FOSS AND FBG-OFDR TECHNOLOGIES**

The previous sections have highlighted research conducted at NASA Dryden to overcome some of the technical barriers to large-scale implementation of FOSS technologies into aerospace vehicle design. The need to overcome the cultural barriers to FOSS acceptance, as articulated in the Introduction, is more critical now than ever before. Trends in the aerospace community towards ultra-lightweight, elastically tailorable long-span structures that can competently fly at higher altitudes for longer durations are forcing aircraft design into new realms without the underpinning of fundamental understanding of physical phenomena. To achieve new mission requirements, Uninhabited Aerial Vehicle (UAV) designs are converging on solutions with hundreds of feet of wing span, requiring the use of non-traditional engineering materials, such as balsa wood and mylar. Thin gage materials cease to perform in a manner consistent with handbook values that were determined with bulk materials. Decoupled, single discipline, linear design, and analysis models are insufficient to address the complexity associated with the new challenges in aerospace vehicle designs. These trends are also growing for transport and commercial aircraft designs with the perennial goals of reducing weight, reducing fuel burn rates, increasing range, and payload capacity.

The benefits of FOSS technology and its potential to address these formidable challenges, make its acceptance by the aerospace community that much more important. The prospect of dramatically improving the measurement count-to-total sensor weight, or data-to-weight ratio has the potential to benefit the vehicle management and operations from early design to final retirement. One recent in-house study estimates that FBG sensors based on OFDR can provide 100 to 1000 times the number of conventional strain/temperature measurements at 1/100 to 1/1000 of the total sensor weight, depending on the application. Conventional technologies and business-as-usual cultural practices and methodologies must be overcome to realize the full potential that the FOSS technologies offer.

To illustrate the potential game-changing benefits of FOSS technology, this section first presents the notion of a vision vehicle. This vision vehicle could represent the state of the art for aircraft designs flying in the next generation. Such a vehicle is first introduced and then the benefits of FOSS at each stage in the vehicle life cycle are described.

### **7.1 THE FOSS VISION VEHICLE**

A FOSS vision vehicle would be instrumented with large arrays of sensor networks analogous to biological systems. These networks would be bonded primarily to the outer external surfaces of the vehicle using efficient, large-scale attachment methods. Other sensors would be incorporated during fabrication on interior structures and embedded within the composite laminate on key components. Comprehensive knowledge of the flight vehicle airframe would be underpinned by a structured build up approach where FOSS sensors would provide unparalleled feedback in all parts of ground test structures, from coupon to qualification unit. Models at each stage of the structural test would be refined and updated by correlating with FOSS measurements. In flight, hundreds of thousands of FBG sensors would provide a litany of measurands; a sub-set of which would be used for feedback control and updating on-board simulations. Sensor mesh densities on the vehicle airframe would be commensurate with the degrees of freedom present with detailed finite-element models. These networks would be judiciously arrayed such that high spatially resolved sensor meshes would exist in areas of non-uniform gradients and lower densities in larger acreage portions with lower gradients. Sensor networks would be defined such that component strains/stresses in multiple directions would be available to determine principal, normal, shear, and von Mises stresses/strains. Mode shapes and buckling modes (eigenvectors) from elastic instabilities could be assessed, and if significant, could be displayed to key personnel by an on-board Structural Health Monitoring System in real time. If catastrophic failure was imminent, such information could be fed to appropriate on-board sub-system

computers to mitigate failure without human intervention. Regions on the aircraft where damage was suspected would be identified and automatically targeted for post-flight non-destructive evaluation and condition-based maintenance.

This section shows how FBG-OFDR sensing technology supports the initial stages of structural design; facilitates new advances in fabrication and manufacturing; reduces time, cost, and complexity of ground test and evaluation; provides real-time structural monitoring capability during nominal and off-nominal flight operations; improves maintenance turn-around times; and provides comprehensive vehicle life predictions for end of life decisions.

## **7.2 DESIGN AND DEVELOPMENT**

A vehicle with FOSS technologies flying in the future could look radically different and have pronounced economic and military benefit than vehicles flying today. Many aspects of vehicle design and development can benefit from FOSS technologies. One key benefit is providing a better fundamental understanding of the complex behavior of future designs. Having high-spatial and temporal physical response feedback throughout the development cycle (from ground test articles to flight structures) would ensure that such a vehicle would have been designed with a better understanding of the fundamental physics that govern such vehicles and the environments in which they fly. This profound understanding would produce comprehensively validated multi-disciplinary physics-based models that will ensure the lightest and most efficient designs possible. Benefits to these optimized tools would be enormous: they will save weight, reduce fuel costs, minimize operating and maintenance costs, and improve overall vehicle performance. Installing thousands of sensors on structural components in faster times and with less personnel would ensure that vehicle development path from sub-component testing to first flight would have been faster and less expensive. Efficient and accurate multi-disciplinary design tools would optimize design margins approaching 1.0 such that excessive weight could be pulled from the vehicle structure. Structural design uncertainty, which drives higher design margins, would be reduced by comprehensive structural feedback at every step of the test program. This feedback would also identify areas where additional strength was required due to under-designed regions, thus ensuring greater safety. These design and analysis tools would have been validated throughout all phases of the structure development process, from the ground (coupons, sub-components, qualification units, flight structures) through the flight envelope expansion process.

Another key benefit of FOSS designs is that in-service performance data can now be feedback to designers who rarely have access to such data to validate their design assumptions. According to a Wall Street Journal report, following the aftermath of a crash of an Alaskan Airlines MD-83 (McDonnell Douglas, now The Boeing Company, Chicago, Illinois) off the coast of Southern California in January 2000, an independent report addressing airline safety found in part that the validity of initial design assumptions was seldom verified by comparison with databases of in service performance. [29] By providing finite-element-like results with these experimental measurements, designers now can evaluate the efficacy of their structural designs and improve their models. Compared to current structural designers, who rarely have more than a handful of strain gage channels to assess structural performance of the entire vehicle, designers of the FOSS vision vehicle have hundreds of thousands of hair-like sensors to validate their design assumptions.

Design tools for the FOSS vision vehicle would be based on a better understanding of the complex airframe response to external environment forces. Current vehicle development efforts focus on building a specific platform for a specific application rather than developing a thorough understanding of the fundamentals associated with vehicle performance. Previous design tools based on linear structural analysis, linear-elastic materials, linear control theory, linear and steady aerodynamic assumptions, and decoupled disciplinary analyses are not acceptable to satisfy current and future aircraft design requirements. The lack of fundamental knowledge of issues directly related to lighter weight designs inhibits fast and efficient development, and safe operation of new UAVs. Such was the case with the in-flight breakup of the Helios UAV (Figure 7-1). The mishap investigation board concluded that for these complex airframes, more accurate, multi-disciplinary,

time domain design and analysis tools were essential for examining the effects of disturbances on the behavior of highly flexible vehicles (Thomas Noll, et al, “Investigation of the Helios Prototype Aircraft Mishap Volume 1 Mishap Report”, NASA internal document, January 2004).



NASA Photo ED01-0209-2



NASA Photo ED03-0180-03

**Figure 7-1: Helios UAV at Take-Off (Left) and In-Flight Break-Up (Right).**

The goal of reducing aircraft weight means that aircraft structures will inherently be more flexible, which translates into greater risk of structural instabilities and adverse coupling between aerodynamic forces and structural response. The fluid-structure interaction problem means that flight control laws must be more robust and able to safely control the vehicle throughout its life. With these vast networks of hair-like sensors, model validation can be accomplished comprehensively. In addition, traditionally crude design assumption regarding gusts, unsteady aero, etc., can be better understood (i.e. yielding weight reductions) and can be placed in regions previously not possible (within bolted joints, embedded within composite structure). Embedded FBGs will increase the physical understanding of curing the process and material system performance during the life of the structure.

### **7.3 FABRICATION AND SENSOR INSTALLATION**

Structural sensors for the FOSS vision vehicle would be efficiently bonded to the vehicle surfaces in large pre-packaged sheets (i.e. SMART Layer, as described in Section 4.3), either during, or immediately following fabrication. These ultra-thin, plastic layers would contain integrated arrays of FBG sensor networks as part of the overall integrated vehicle design. FBG sensor networks could also be embedded with the composite airframe during the fabrication process. The sensor sheets could result in the installation of thousands of sensors in a fraction of the time required for conventional and FBG sensors today. These integrated packaged layers may also further minimize the already nearly negligible geometric disturbances that the small fibers might cause.

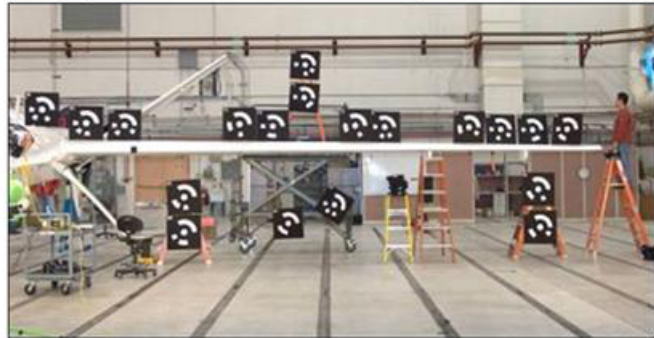
### **7.4 GROUND TESTING**

Despite the increasing complexity of future aircraft designs, the FOSS vision vehicle should be able to achieve first flight in a fraction of the time it takes for current vehicle designs. Schedule reductions should result from more efficient test techniques afforded by vast numbers of surface-mounted sensors operating in conjunction with real-time structural models. New ground test techniques using fiber optic sensors have the potential to reduce the test complexity and increase a greater understanding of physical response of the airframe throughout ground testing.

Figure 7-1 shows the complexity of current ground test techniques compared to the simplicity of ground tests conducted with fiber optic sensor arrays. Figure 7-2 shows a typical strain gage loads calibration being conducted on the Northrop Grumman (Falls Church, Virginia) E2C Hawkeye. These tests required 16 channels of load actuation to apply an array of mechanical loads in order to determine stiffness coefficients for strain-gage-based loads equations. These equations are required to monitor the flight loads produced on the airframe during a conventional flight research program. To monitor the flight loads, dozens of strain gage channels had to be installed on the interior load bearing structures in the wing. Wing skins had to be removed and strain gages and thermocouples had to be installed. Typical installation times for foil strain gages are approximately 4 hours per gage.



NASA Photo EC04-0360-1192



NASA Photo ED08-0016-12

**Figure 7-2: Traditional Strain Gage Loads Calibration Testing in NASA Dryden's Flight Loads Lab, and Simplified Tests for Determining Structural Properties of as Built Structures and Real Time in Flight Loads.**

The FOSS vision is to perform ground tests in fractions of the time, saving time at all phases of the test program. During the instrumentation phase, a few fiber channels, each containing thousands of sensors can be hooked up, checked out, and identified in much shorter time than with conventional strain and temperature sensors. Conventional strain sensors require one channel per sensor. As shown previously, the number of instrumentation channels is significantly reduced with a few small fibers.

The other advantage of FBG instrumented structures is that these sensors are small enough that they can be installed at high-lift locations on the aircraft. Conventional strain gage technology is too massive and perturbative to be placed in these high lift regions. Because of their small size, FBG sensors can also remain on the structure throughout the vehicle life cycle, unlike other ground-test-specific instrumentation that has to be removed prior to flight. Therefore, extra time is required before and after testing to both install and remove instrumentation required for ground testing.

## **7.5 FLIGHT OPERATIONS**

### **7.5.1 Nominal Flight**

Perhaps the greatest benefit of the FOSS technology is realized when the FOSS vision vehicle performs its mission in the actual flight environment. The efficient ultra-light airframe design, enabled by FOSS technologies is now able to save hundreds of millions of dollars of fuel per year for the entire inventory of FOSS vehicles in commercial and military fleets. The shape of the wings and tails of the vehicle are well known and can be used in combination with the conventional control surfaces to more optimally tune the wings in-flight to improve aerodynamic performance. Advances in actuator technology enable the aeroelastic control of the aerodynamic surfaces to increase lift, reduce drag, and redistribute aerodynamic loads to regions having greater load bearing capacity. A few percent increase in aerodynamic efficiency

allows the FOSS vision vehicle to travel further and carry more cargo and passengers than previous generations of aircraft designs. The ability to determine many real-time parameters opens up the prospect for future vehicles to perform real-time simulations. Data driven simulations can be used to predict near-term vehicle response to changes in flight environment, such as weather conditions. Real-time on-board data driven simulations can also be used to update control laws for a variety of scenarios, such as loss of control surface that might occur due to battle damage or lightning strikes.

The FOSS vision vehicle is equipped with a real-time health monitoring system that can provide thousands of engineering parameters to monitor and manage vehicle health. FBG sensors can be placed on high-pressure and extreme temperature tanks, hoses, and cables to monitor system health. These sensors can be placed on and embedded within Composite Over-Wrapped Pressure Vessels (COPVs) to monitor the health of these vessels and avoid stress rupture. The monitoring of COPVs is a current topic of a considerable amount of research within NASA. Overloading of key structural components can be monitored and four-dimensional mapping (three spatial-coordinates and time) will provide accurate assessment of system and structural health. With the highly resolved mapping capability, the FOSS structures can pinpoint areas for post-flight inspection. Condition-based, rather than time-based maintenance can now be better achieved.

### **7.5.2 Off-Nominal Flight**

Another significant benefit to FOSS technologies is the ability for the FOSS vision vehicle to make real-time adjustments to mission plans based on sensory feedback. On-board simulations can be performed and models can be validated for sudden changes in aircraft performance due to control surface malfunction or damage. Sudden changes in atmospheric conditions, such as increased turbulence and wind shear can be addressed with FOSS-facilitated gust-alleviation techniques. With sensor networks on FOSS structures, other unexpected and dramatic changes in external environment such as buffeting can be handled effectively. In order to prevent elastic instabilities such as buckling and flutter, FOSS structures along with advanced materials and actuators can effectively control mode shapes and buckled regions. By maintaining orthogonal mode shapes to prevent off-diagonal interactions in the mode shapes, flutter can be suppressed for FOSS vision vehicles of the future.

For other off-nominal flight conditions, FOSS technology also has the potential to avoid truly catastrophic results of loss of life, loss of mission, and loss of assets. When aircraft systems suffer in-air emergencies, having validated information is always indispensable in determining the most appropriate remediation strategy. For missions in which assets are deployed for long periods of time, such as HALE missions and space exploration, off-nominal emergencies can be difficult to overcome. Validated data from sensors covering the vehicle with a few dozen fibers could prove to be the difference between mission success and failure.

## **7.6 END OF LIFE DECISION MAKING**

Finally, at the later stages of aircraft service, the question remains as to how much longer an aircraft can remain in service and safely fulfill its mission. As military and civilian budgets become smaller, military and civilian aircraft are more commonly expected to be used well beyond their service lives. Sampath, for example, notes that in 1993, 51 percent of U.S. Air Force inventory was 15 years and older, while 44 percent were over 20 years old. [30] The problem is further exacerbated by shrinking budgets that require many of these aircraft to continue fleet service for years beyond their design life. The more these vehicles fly beyond their design life, the higher maintenance costs become. The scheduled inspection and repair of each EF-11A (General Dynamics, now the Lockheed Martin Corporation, Bethesda, Maryland) aircraft in the depot had risen from 2200 hours in 1985, to 8000 hours in 1996. [30] The problem of aging aircraft, similar to that of an aging family car, is that issues of maintenance and operational expense become a serious budgetary concern. FOSS structures have been envisioned by many as the mechanism to

## THE FUTURE OF FOSS AND FBG-OFDR TECHNOLOGIES

---

help alleviate such problems. The ability to provide real-time continuous structural health management of fleet aircraft and aerospace vehicles is envisioned to dramatically reduce operational and maintenance costs, and thus allow these vehicles and structures to extend their service lives.

A clear example of the consequence of using aircraft beyond their safe life occurs when the U.S. Air Force decommissions fleet aircraft. Agencies such as the U.S. Forest Service are able to retro fit these aircraft to support their mission. With these conventional airframes, there is a serious lack of detailed knowledge to accurately predict the remaining fatigue life in these structures. Figure 7-3 shows the in-flight catastrophe of such an aircraft. This Forest Service aircraft experienced a catastrophic wing structure failure on this C-130 (Lockheed Martin Corporation, Bethesda, Maryland) while performing a mission in 2002. The U.S. Air Force placed the aircraft in service in 1957. Future FOSS airframes can be certified for future use because they have the ability to use data driven models to facilitate end-of-service life decisions, such as those discussed in earlier.



**Figure 7-3: B52 Aircraft Boneyard (Left), and Video Capture of an In-Flight Structural Failure of a C-130A (Right).**

## Chapter 8 – CONCLUSIONS

This paper presented an overview of the research and technology development performed at NASA Dryden in support of fiber optic sensory structures development. Merits and theory of FBG sensor technology, as well as optical frequency domain reflectometry were presented to provide a fundamental understanding of the technical benefits that can be realized by the aerospace community in placing FOSS technology into service. FBG technology as implemented with an optical frequency domain reflectometry can provide thousands of measurements with virtually no added weight. These sensors are lightweight, about the size of a human hair, and can be multiplexed; thousands of sensors can be supported with a few small fibers. The sensors are also small enough to be placed on the outer moldline of lifting surfaces without negligible impact to flow field quality.

Both ground and flight systems have been developed and flight validated, FBG sensors have been characterized and attachment methods have been developed. One of the powerful aspects of this new sensor technology is that they can be used in conjunction with data driven structural transfer functions. This approach opens up new areas of research by gaining a more comprehensive understanding of both the internal loads obtained in response to the external forces that act upon FOSS airframes. Strain, temperature, wing shape, structural displacements, external loads, structural and material properties, and fatigue life are just a sampling of engineering parameters that can be accurately determined using these highly multiplexed sensor systems.

Recent examples of large-scale application of FOSS technologies were presented. Such examples included the strain and wing shape validation testing performed on NASA's Predator B UAV, called Ikhana. Large-scale ground testing was also performed on NESC's CCM. FBG sensors were placed around the perimeter of windows and the hatch to measure strain gradients around these regions. Ground and flight-test systems have also been deployed on the Global Observer UAV and data acquired to validate aircraft designs.

Lastly, the future role and vision of FBG, OFDR, and FOSS technologies was explored to further highlight the potential positive impact that these technologies can have in aerospace vehicle design. Each phase of the vehicle life cycle was evaluated through the use of a FOSS vision vehicle of the future. From vehicle concept to retirement, FOSS technology can increase fundamental understanding of aerospace vehicle performance with virtually no penalty, and thereby reduce airframe weight, intelligently adapt to both internal and external conditions, reduce costs, improve performance, increase range, and increase cargo and passenger capacity.

## CONCLUSIONS

---





## Chapter 9 – REFERENCES

- [1] Udd, E., Ed., “Fiber Optic Sensors: An Introduction for Engineers and Scientists”, New York, NY, USA, John Wiley & Sons, Inc., 1991, p. 171.
- [2] Van Steenkiste, R.J. and Springer, G.S., “Strain and Temperature Measurement with Fiber Optic Sensors”, Lancaster, PA, USA, Technomic Publishing Company, 1997.
- [3] Udd, E., Ed., “Fiber Optic Smart Structures”, New York, NY, USA, John Wiley & Sons, Inc., 1995, p. 172.
- [4] Measures, R.M., “Structural Monitoring with Fiber Optic Technology”, London, Academic Press, 2001.
- [5] Staszewski, W.J., Boller, C. and Tomlinson, G.R., Eds., “Health Monitoring of Aerospace Structures”, Chichester, UK, John Wiley & Sons, 2003.
- [6] Richards, W.L., Parker, A.R. Jr., Ko, W.L. and Piazza, A., “Fiber Optic Strain and Wing Shape Sensing on a Modified Predator-B Unmanned Aerial Vehicle”, SPIE Defense Security and Sensing, Orlando, FA, USA, April 15, 2009.
- [7] Schweikhard, K., Richards, W.L., Theisen, J., Mouyos, W. and Garbos, R., “Flight Demonstration of X-33 Vehicle Health Management Systems Components on the F/A-18 Systems Research Aircraft”, NASA/TM-2001-209037, November 2001.
- [8] Emmons, M.C., Karnani, S., Trono, S., Mohanchandra, K.P., Carman, G.P. and Richards, W.L., “Characterization of Optical Fiber Bragg Gratings as Strain Sensors Considering Load Direction”, Ellicott City, MD, USA, ASME Smart Materials, Adaptive Structures and Intelligent Systems, October 28-30, 2008.
- [9] Emmons, M.C., Karnani, S., Trono, S., Mohanchandra, K.P., Richards, W.L. and Carman, G.P., “Strain Measurement Validation of Embedded Fiber Bragg Gratings”, International Journal of Optomechatronics, 2010, Vol. 4, No. 1, pp. 22-33.
- [10] Othonos, A., “Fiber Bragg gratings”, Review of Scientific Instruments, 1997, Vol. 68, No. 12, pp. 4309-4341.
- [11] Dally, J.W. and Riley, W.F., “Experimental Stress Analysis, 3<sup>rd</sup> Edition”, New York, McGraw-Hill, Inc., 1991 (ISBN 0-07-015218-7).
- [12] Froggatt, M. and Moore, J., “Distributed Measurement of Static Strain in an Optical Fiber with Multiple Bragg Gratings at Nominally Equal Wavelengths”, Applied Optics, 1998, Vol. 37, No. 10, pp. 1741-1746.
- [13] Froggatt, M., “Apparatus and Method for Measuring Strain in Bragg Gratings”, U.S. Patent 5,798,521, 1998.
- [14] Sirkis, J.S., “Fiber Optic Sensors for Smart Structures: Basics and Applications”, SPIE’s 5<sup>th</sup> Annual International Symposium on Smart Structures and Materials, March 1-5, 1998.
- [15] Anon., “Errors Due to Transverse Sensitivity in Strain Gages”, Measurements Group, Inc. TN-509, 1982.

## REFERENCES

---

- [16] Anon., "Temperature-Induced Apparent Strain and Gage Factor Variation in Strain Gages", Measurements Group, Inc., TN-504, 1983, pp. 1-7.
- [17] Williams, W.D., Lei, J.F., Reardon, L.F., Krake, K., Lemcoe, M.M., Holmes, H.K. and Moore Sr., T.C., "High-Temperature Strain Sensor and Mounting Development", NASA TP 3540, December 1996.
- [18] Richards, W.L., "A New Strain Correction Technique for Strain Gage Measurements Acquired in Transient Temperature Environments", NASA TP 3593, March 1996.
- [19] Hu, J.-Q., Beard, S., Qing, X.P., Li, I., Piazza, A. and Richards, W.L., "FBG Sensor Installation and Integration Using SMART Layer Technologies for Aerospace Applications", International Workshop on Structural Health Monitoring (IWSHM), Stanford, CA, USA, 2009.
- [20] Ko, W.L. and Richards, W.L., "Method for Real-Time Structure Shape-Sensing", U.S. Patent No. 7,520,176, April 21, 2009.
- [21] Ko, W.L., Richards, W.L. and Fleischer, V.T., "Displacement Theories for In-Flight Deformed Shape Predictions of Aerospace Structures", NASA/TP-2007-214612, October 2007.
- [22] Ko, W.L., Richards, W.L. and Fleischer, V.T., "Applications of Ko Displacement Theory to the Deformed Shape Predictions of Doubly Tapered Ikhana Wing", NASA/TP-2009-214652, November 2009.
- [23] Ko, W.L. and Fleischer, V.T., "Further Development of Ko Displacement Theory for Deformed Shape Predictions of Non-Uniform Aerospace Structures", NASA/TP 2009-214643, September 2009.
- [24] Jutte, C.V., Ko, W.L., Stephens, C.A., Bakalyar, J.A., Richards, W.L. and Parker, A.R., "Deformed Shape Calculation of a Full-Scale Wing Using Fiber Optic Strain Data from a Ground Loads Test", NASA/TP-2011-215975, December 2011.
- [25] Moore, J. and Rogge, M., "Method and Apparatus for Shape and End Position Determination Using an Optical Fiber", U.S. Patent No. 7,813,599, August 2010.
- [26] Richards, W.L. and Ko, W.L., "Process for Using Surface Strain Measurements to Obtain Operational Loads for Complex Structures", U.S. Patent, 7,715,994, May 2010.
- [27] Ko, W.L., Tran, V.T. and Chen, T., "Incorporation of Half-Cycle Theory into Ko Aging Theory for Aero-Structural Flight- Life Predictions", NASA/TP-2007-214608, January 2007.
- [28] Ko, W.L. and Chen, T., "Extended Aging Theories for Predictions of Safe Operational Life of Critical Airborne Structural Components", NASA/TM-2006-213676, March 2006.
- [29] Pasztor, A., "FAA to Change Way it Assesses Aircraft Safety", The Wall Street Journal, March 21, 2002, p. A3.
- [30] Sampath, S.G., "Aging Combat Aircraft Fleets – Long Term Applications: Introduction to Lecture Series", AGARD LS-206, 1996, p. I1- I3.

## **Annex A – AGARD and RTO Flight Test Instrumentation and Flight Test Techniques Series**

### **1. Volumes in the AGARD and RTO Flight Test Instrumentation Series, AGARDograph 160**

Volume Number	Title	Publication Date
1.	Basic Principles of Flight Test Instrumentation Engineering (Issue 2) Issue 1: Edited by A. Pool and D. Bosman Issue 2: Edited by R. Borek and A. Pool	1974 1994
2.	In-Flight Temperature Measurements by F. Trenkle and M. Reinhardt	1973
3.	The Measurements of Fuel Flow by J.T. France	1972
4.	The Measurements of Engine Rotation Speed by M. Vedrunes	1973
5.	Magnetic Recording of Flight Test Data by G.E. Bennett	1974
6.	Open and Closed Loop Accelerometers by I. McLaren	1974
7.	Strain Gauge Measurements on Aircraft by E. Kottkamp, H. Wilhelm and D. Kohl	1976
8.	Linear and Angular Position Measurement of Aircraft Components by J.C. van der Linden and H.A. Mensink	1977
9.	Aeroelastic Flight Test Techniques and Instrumentation by J.W.G. van Nunen and G. Piazzoli	1979
10.	Helicopter Flight Test Instrumentation by K.R. Ferrell	1980
11.	Pressure and Flow Measurement by W. Wuest	1980
12.	Aircraft Flight Test Data Processing – A Review of the State of the Art by L.J. Smith and N.O. Matthews	1980
13.	Practical Aspects of Instrumentation System Installation by R.W. Borek	1981
14.	The Analysis of Random Data by D.A. Williams	1981
15.	Gyroscopic Instruments and Their Application to Flight Testing by B. Stieler and H. Winter	1982
16.	Trajectory Measurements for Take-off and Landing Test and Other Short-Range Applications by P. de Benque D'Agut, H. Riebeek and A. Pool	1985

17.	Analogue Signal Conditioning for Flight Test Instrumentation by D.W. Veatch and R.K. Bogue	1986
18.	Microprocessor Applications in Airborne Flight Test Instrumentation by M.J. Prickett	1987
19.	Digital Signal Conditioning for Flight Test by G.A. Bever	1991
20.	Optical Air Flow Measurements in Flight by R.K. Bogue and H.W. Jentink	2003
21.	Differential Global Positioning System (DGPS) for Flight Testing by R. Sabitini and G.B. Palmerini	2008
22.	Application of Fiber Optic Instrumentation by W.L. Richards, A.R. Parker Jr., W.L. Ko, A. Piazza and P. Chan	2012

## 2. Volumes in the AGARD and RTO Flight Test Techniques Series

Volume Number	Title	Publication Date
AG237	Guide to In-Flight Thrust Measurement of Turbojets and Fan Engines by the MIDAP Study Group (UK)	1979
The remaining volumes are published as a sequence of Volume Numbers of AGARDograph 300.		
1.	Calibration of Air-Data Systems and Flow Direction Sensors by J.A. Lawford and K.R. Nippres	1988
2.	Identification of Dynamic Systems by R.E. Maine and K.W. Iliff	1988
3.	Identification of Dynamic Systems – Applications to Aircraft Part 1: The Output Error Approach by R.E. Maine and K.W. Iliff	1986
	Part 2: Nonlinear Analysis and Manoeuvre Design by J.A. Mulder, J.K. Sridhar and J.H. Breeman	1994
4.	Determination of Antenna Patterns and Radar Reflection Characteristics of Aircraft by H. Bothe and D. McDonald	1986
5.	Store Separation Flight Testing by R.J. Arnold and C.S. Epstein	1986
6.	Developmental Airdrop Testing Techniques and Devices by H.J. Hunter	1987
7.	Air-to-Air Radar Flight Testing by R.E. Scott	1992
8.	Flight Testing under Extreme Environmental Conditions by C.L. Henrickson	1988
9.	Aircraft Exterior Noise Measurement and Analysis Techniques by H. Heller	1991
10.	Weapon Delivery Analysis and Ballistic Flight Testing by R.J. Arnold and J.B. Knight	1992
11.	The Testing of Fixed Wing Tanker & Receiver Aircraft to Establish Their Air-to-Air Refuelling Capabilities by J. Bradley and K. Emerson	1992
12.	The Principles of Flight Test Assessment of Flight-Safety-Critical Systems in Helicopters by J.D.L. Gregory	1994
13.	Reliability and Maintainability Flight Test Techniques by J.M. Howell	1994
14.	Introduction to Flight Test Engineering Issue 1: Edited by F. Stoliker Issue 2: Edited by F. Stoliker and G. Bever	1995 2005
15.	Introduction to Avionics Flight Test by J.M. Clifton	1996

16.	Introduction to Airborne Early Warning Radar Flight Test by J.M. Clifton and F.W. Lee	1999
17.	Electronic Warfare Test and Evaluation by H. Banks and R. McQuillan	2000
18.	Flight Testing of Radio Navigation Systems by H. Bothe and H.J. Hotop	2000
19.	Simulation in Support of Flight Testing by D. Hines	2000
20.	Logistics Test and Evaluation in Flight Testing by M. Bourcier	2001
21.	Flying Qualities Flight Testing of Digital Flight Control Systems by F. Webster and T.D. Smith	2001
22.	Helicopter/Ship Qualification Testing by D. Carico, R. Fang, R.S. Finch, W.P. Geyer Jr., Cdr. (Ret.) H.W. Krijns and K. Long	2002
23.	Flight Test Measurement Techniques for Laminar Flow by D. Fisher, K.H. Horstmann and H. Riedel	2003
24.	Precision Airdrop by M.R. Wuest and R.J. Benney	2005
25.	Flight Testing of Night Vision Systems in Rotorcraft by G. Craig, T. Macuda, S. Jennings, G. Ramphal and A. Stewart	2007 <sup>†</sup>
26.	Airborne Laser Systems Testing and Analysis by R. Sabatini and M.A. Richardson	2010
27.	Unique Aspects of Flight Testing Unmanned Aircraft Systems by A.E. Pontzer, M.D. Lower and J.R. Miller	2010

At the time of publication of the present volume, the following volumes are in preparation:

Electronic Warfare Test and Evaluation (expected August 2012)

Safety and Risk Management in Flight Testing (expected December 2013)

Aircraft Stores Compatibility, Integration, and Separation Testing (expected December 2014)

Reduced Friction Runway Surface Flight Testing (expected December 2014)

High Altitude Rotary Wing Flight Testing (expected December 2015)

---

<sup>†</sup> Volume 25 has been published as RTO AGARDograph AG-SCI-089.

<b>REPORT DOCUMENTATION PAGE</b>			
<b>1. Recipient's Reference</b>	<b>2. Originator's References</b>	<b>3. Further Reference</b>	<b>4. Security Classification of Document</b>
	RTO-AG-160 AC/323(SCI-228)TP/446 Volume 22	ISBN 978-92-837-0164-4	UNCLASSIFIED/ UNLIMITED
<b>5. Originator</b>			
Research and Technology Organisation North Atlantic Treaty Organisation BP 25, F-92201 Neuilly-sur-Seine Cedex, France			
<b>6. Title</b>			
Application of Fiber Optic Instrumentation			
<b>7. Presented at/Sponsored by</b>			
SCI-228, the Flight Test Technology Task Group of the Systems Concepts and Integration Panel (SCI) of RTO.			
<b>8. Author(s)/Editor(s)</b>			<b>9. Date</b>
Dr. W. Lance Richards, Ph. D., Mr. Allen R. Parker, Jr., Dr. William L. Ko, Ph. D., Mr. Anthony Piazza and Dr. Patrick Chan, Ph. D.			July 2012
<b>10. Author's/Editor's Address</b>			<b>11. Pages</b>
Dryden Flight Research Center, P.O. Box 273, Edwards, California 93523, USA			66
<b>12. Distribution Statement</b>			
There are no restrictions on the distribution of this document. Information about the availability of this and other RTO unclassified publications is given on the back cover.			
<b>13. Keywords/Descriptors</b>			
Fiber optics Flight test instrumentation Strain sensing Structural analysis Test techniques			
<b>14. Abstract</b>			
<p>Fiber optic sensing technology has emerged in recent years offering tremendous advantages over conventional aircraft instrumentation systems. The advantages of fiber optic sensors over their conventional counterparts are well established; they are lighter, smaller, and can provide enormous numbers of measurements at a fraction of the total sensor weight. After a brief overview of conventional and fiber-optic sensing technology, this paper presents an overview of the research that has been conducted at NASA Dryden Flight Research Center in recent years to advance this promising new technology. Research and development areas include system and algorithm development, sensor characterization and attachment, and real-time experimentally-derived parameter monitoring for ground- and flight-based applications. The vision of fiber optic smart structure technology is presented and its potential benefits to aerospace vehicles throughout the lifecycle, from preliminary design to final retirement, are presented.</p>			







BP 25

F-92201 NEUILLY-SUR-SEINE CEDEX • FRANCE  
Télécopie 0(1)55.61.22.99 • E-mail [mailbox@rta.nato.int](mailto:mailbox@rta.nato.int)

**DIFFUSION DES PUBLICATIONS****RTO NON CLASSIFIEES**

Les publications de l'AGARD et de la RTO peuvent parfois être obtenues auprès des centres nationaux de distribution indiqués ci-dessous. Si vous souhaitez recevoir toutes les publications de la RTO, ou simplement celles qui concernent certains Panels, vous pouvez demander d'être inclus soit à titre personnel, soit au nom de votre organisation, sur la liste d'envoi.

Les publications de la RTO et de l'AGARD sont également en vente auprès des agences de vente indiquées ci-dessous.

Les demandes de documents RTO ou AGARD doivent comporter la dénomination « RTO » ou « AGARD » selon le cas, suivi du numéro de série. Des informations analogues, telles que le titre et la date de publication sont souhaitables.

Si vous souhaitez recevoir une notification électronique de la disponibilité des rapports de la RTO au fur et à mesure de leur publication, vous pouvez consulter notre site Web ([www.rto.nato.int](http://www.rto.nato.int)) et vous abonner à ce service.

**CENTRES DE DIFFUSION NATIONAUX****ALLEMAGNE**

Streitkräfteamt / Abteilung III  
Fachinformationszentrum der Bundeswehr (FIZBw)  
Gorch-Fock-Straße 7, D-53229 Bonn

**BELGIQUE**

Royal High Institute for Defence – KHID/IRSD/RHID  
Management of Scientific & Technological Research  
for Defence, National RTO Coordinator  
Royal Military Academy – Campus Renaissance  
Renaissancelaan 30, 1000 Bruxelles

**CANADA**

DSIGRD2 – Bibliothécaire des ressources du savoir  
R et D pour la défense Canada  
Ministère de la Défense nationale  
305, rue Rideau, 9<sup>e</sup> étage  
Ottawa, Ontario K1A 0K2

**DANEMARK**

Danish Acquisition and Logistics Organization (DALO)  
Lautrupbjerg 1-5, 2750 Ballerup

**ESPAGNE**

SDG TECIN / DGAM  
C/ Arturo Soria 289  
Madrid 28033

**ESTONIE**

Estonian Ministry of Defence  
Estonian National Coordinator for NATO RTO  
Sakala 1, Tallinn 15094

**ETATS-UNIS**

NASA Center for AeroSpace Information (CASI)  
7115 Standard Drive  
Hanover, MD 21076-1320

**FRANCE**

O.N.E.R.A. (ISP)  
29, Avenue de la Division Leclerc  
BP 72, 92322 Châtillon Cedex

**GRECE (Correspondant)**

Defence Industry & Research General  
Directorate, Research Directorate  
Fakinos Base Camp, S.T.G. 1020  
Holargos, Athens

**HONGRIE**

Hungarian Ministry of Defence  
Development and Logistics Agency  
P.O.B. 25, H-1885 Budapest

**ITALIE**

General Secretariat of Defence and  
National Armaments Directorate  
5<sup>th</sup> Department – Technological  
Research  
Via XX Settembre 123, 00187 Roma

**LUXEMBOURG**

Voir Belgique

**NORVEGE**

Norwegian Defence Research  
Establishment, Attn: Biblioteket  
P.O. Box 25  
NO-2007 Kjeller

**PAYS-BAS**

Royal Netherlands Military  
Academy Library  
P.O. Box 90.002  
4800 PA Breda

**POLOGNE**

Centralna Biblioteka Wojskowa  
ul. Ostrobramska 109  
04-041 Warszawa

**PORTUGAL**

Estado Maior da Força Aérea  
SDFCA – Centro de Documentação  
Alfragide, P-2720 Amadora

**REPUBLIQUE TCHEQUE**

LOM PRAHA s. p.  
o. z. VTÚLaPVO  
Mladoboleslavská 944  
PO Box 18  
197 21 Praha 9

**ROUMANIE**

Romanian National Distribution  
Centre  
Armaments Department  
9-11, Drumul Taberei Street  
Sector 6  
061353, Bucharest

**ROYAUME-UNI**

Dstl Knowledge and Information  
Services  
Building 247  
Porton Down  
Salisbury SP4 0JQ

**SLOVAQUIE**

Akadémia ozbrojených síl gen.  
M.R. Štefánika, Distribučné a  
informačné stredisko RTO  
Demänová 393, Liptovský Mikuláš 6  
031 06

**SLOVENIE**

Ministry of Defence  
Central Registry for EU and  
NATO  
Vojkova 55  
1000 Ljubljana

**TURQUIE**

Milli Savunma Bakanlığı (MSB)  
ARGE ve Teknoloji Dairesi  
Başkanlığı  
06650 Bakanlıklar  
Ankara

**AGENCES DE VENTE****NASA Center for AeroSpace Information (CASI)**

7115 Standard Drive  
Hanover, MD 21076-1320  
ETATS-UNIS

**The British Library Document Supply Centre**

Boston Spa, Wetherby  
West Yorkshire LS23 7BQ  
ROYAUME-UNI

**Canada Institute for Scientific and Technical Information (CISTI)**

National Research Council Acquisitions  
Montreal Road, Building M-55  
Ottawa K1A 0S2, CANADA

Les demandes de documents RTO ou AGARD doivent comporter la dénomination « RTO » ou « AGARD » selon le cas, suivie du numéro de série (par exemple AGARD-AG-315). Des informations analogues, telles que le titre et la date de publication sont souhaitables. Des références bibliographiques complètes ainsi que des résumés des publications RTO et AGARD figurent dans les journaux suivants :

**Scientific and Technical Aerospace Reports (STAR)**

STAR peut être consulté en ligne au localisateur de ressources uniformes (URL) suivant: <http://ntrs.nasa.gov/search.jsp>  
STAR est édité par CASI dans le cadre du programme NASA d'information scientifique et technique (STI)  
NASA Langley Research Center, STI Program Office, MS 157A  
Hampton, Virginia 23681-0001  
ETATS-UNIS

**Government Reports Announcements & Index (GRA&I)**

publié par le National Technical Information Service  
Springfield  
Virginia 2216  
ETATS-UNIS  
(accessible également en mode interactif dans la base de données bibliographiques en ligne du NTIS, et sur CD-ROM)



BP 25

F-92201 NEUILLY-SUR-SEINE CEDEX • FRANCE  
Télécopie 0(1)55.61.22.99 • E-mail [mailbox@rta.nato.int](mailto:mailbox@rta.nato.int)



**DISTRIBUTION OF UNCLASSIFIED  
RTO PUBLICATIONS**

AGARD & RTO publications are sometimes available from the National Distribution Centres listed below. If you wish to receive all RTO reports, or just those relating to one or more specific RTO Panels, they may be willing to include you (or your Organisation) in their distribution.

RTO and AGARD reports may also be purchased from the Sales Agencies listed below.

Requests for RTO or AGARD documents should include the word 'RTO' or 'AGARD', as appropriate, followed by the serial number. Collateral information such as title and publication date is desirable.

If you wish to receive electronic notification of RTO reports as they are published, please visit our website ([www.rto.nato.int](http://www.rto.nato.int)) from where you can register for this service.

**NATIONAL DISTRIBUTION CENTRES**

**BELGIUM**

Royal High Institute for Defence – KHID/IRSD/RHID  
Management of Scientific & Technological Research  
for Defence, National RTO Coordinator  
Royal Military Academy – Campus Renaissance  
Renaissancelaan 30  
1000 Brussels

**CANADA**

DRDKIM2 – Knowledge Resources Librarian  
Defence R&D Canada  
Department of National Defence  
305 Rideau Street, 9<sup>th</sup> Floor  
Ottawa, Ontario K1A 0K2

**CZECH REPUBLIC**

LOM PRAHA s. p.  
o. z. VTÚLaPVO  
Mladoboleslavská 944  
PO Box 18  
197 21 Praha 9

**DENMARK**

Danish Acquisition and Logistics Organization  
(DALO)  
Lautrupbjerg 1-5  
2750 Ballerup

**ESTONIA**

Estonian Ministry of Defence  
Estonian National Coordinator for NATO RTO  
Sakala 1, Tallinn 15094

**FRANCE**

O.N.E.R.A. (ISP)  
29, Avenue de la Division Leclerc  
BP 72, 92322 Châtillon Cedex

**GERMANY**

Streitkräfteamt / Abteilung III  
Fachinformationszentrum der Bundeswehr (FIZBw)  
Gorch-Fock-Straße 7  
D-53229 Bonn

**GREECE (Point of Contact)**

Defence Industry & Research General  
Directorate, Research Directorate  
Fakinos Base Camp, S.T.G. 1020  
Hologos, Athens

**HUNGARY**

Hungarian Ministry of Defence  
Development and Logistics Agency  
P.O.B. 25, H-1885 Budapest

**ITALY**

General Secretariat of Defence and  
National Armaments Directorate  
5<sup>th</sup> Department – Technological  
Research  
Via XX Settembre 123, 00187 Roma

**LUXEMBOURG**

See Belgium

**NETHERLANDS**

Royal Netherlands Military  
Academy Library  
P.O. Box 90.002  
4800 PA Breda

**NORWAY**

Norwegian Defence Research  
Establishment, Attn: Biblioteket  
P.O. Box 25  
NO-2007 Kjeller

**POLAND**

Centralna Biblioteka Wojskowa  
ul. Ostrobramska 109  
04-041 Warszawa

**PORTUGAL**

Estado Maior da Força Aérea  
SDFA – Centro de Documentação  
Alfragide, P-2720 Amadora

**ROMANIA**

Romanian National Distribution  
Centre  
Armaments Department  
9-11, Drumul Taberei Street  
Sector 6, 061353, Bucharest

**SLOVAKIA**

Akadémia ozbrojených síl gen.  
M.R. Štefánika, Distribučné a  
informačné stredisko RTO  
Demänová 393, Liptovský Mikuláš 6  
031 06

**SLOVENIA**

Ministry of Defence  
Central Registry for EU & NATO  
Vojkova 55  
1000 Ljubljana

**SPAIN**

SDG TECIN / DGAM  
C/ Arturo Soria 289  
Madrid 28033

**TURKEY**

Milli Savunma Bakanlığı (MSB)  
ARGE ve Teknoloji Dairesi  
Başkanlığı  
06650 Bakanlıklar – Ankara

**UNITED KINGDOM**

Dstl Knowledge and Information  
Services  
Building 247  
Porton Down  
Salisbury SP4 0JQ

**UNITED STATES**

NASA Center for AeroSpace  
Information (CASI)  
7115 Standard Drive  
Hanover, MD 21076-1320

**SALES AGENCIES**

**NASA Center for AeroSpace  
Information (CASI)**

7115 Standard Drive  
Hanover, MD 21076-1320  
UNITED STATES

**The British Library Document  
Supply Centre**

Boston Spa, Wetherby  
West Yorkshire LS23 7BQ  
UNITED KINGDOM

**Canada Institute for Scientific and  
Technical Information (CISTI)**

National Research Council Acquisitions  
Montreal Road, Building M-55  
Ottawa K1A 0S2, CANADA

Requests for RTO or AGARD documents should include the word 'RTO' or 'AGARD', as appropriate, followed by the serial number (for example AGARD-AG-315). Collateral information such as title and publication date is desirable. Full bibliographical references and abstracts of RTO and AGARD publications are given in the following journals:

**Scientific and Technical Aerospace Reports (STAR)**

STAR is available on-line at the following uniform resource

locator: <http://ntrs.nasa.gov/search.jsp>

STAR is published by CASI for the NASA Scientific  
and Technical Information (STI) Program

NASA Langley Research Center, STI Program Office, MS 157A  
Hampton, Virginia 23681-0001  
UNITED STATES

**Government Reports Announcements & Index (GRA&I)**

published by the National Technical Information Service

Springfield

Virginia 2216

UNITED STATES

(also available online in the NTIS Bibliographic Database  
or on CD-ROM)